Geoderma 451 (2024) 117081

Contents lists available at ScienceDirect

Geoderma

journal homepage: www.elsevier.com/locate/geoderma

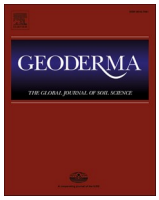

Influence of parent material mineralogy on forest soil nutrient release rates across a nutrient richness gradient

Alexandrea M. Rice [a,1,*], Nicolas Perdrial [b,c], Victoria Treto [b], Anthony W. D'Amato [c], Grace A. Smith [c], Justin B. Richardson [a,1]

[a] Department of Environmental Sciences, University of Virginia, VA, USA
[b] Department of Geography and Geosciences, University of Vermont, Burlington, VT, USA
[c] Rubenstein School of Environment and Natural Resources, University of Vermont, Burlington, VT, USA

ARTICLE INFO

Handling Editor: D. Said-Pullicino

Keywords:
Soil nutrient profiles
Soil weathering
Ca and Mg richness gradient
Soil physicochemical characteristics

ABSTRACT

The influence of parent material mineralogy on nutrient release rates in wood production forests remains poorly understood, despite its importance for sustainable forest management. This study investigated how parent material mineralogy impacts soil nutrient abundance and release rates. We studied three forests in Vermont and New Hampshire across a Ca and Mg richness gradient within the soil parent material. We found that both exchangeable and total nutrient concentrations followed the nutrient richness gradient with exchangeable Ca concentrations highest at the rich (758 mg/kg) and lowest at the poor (51.3 mg/kg) sites. Exchangeable Mg concentrations were higher at the rich (41.5 mg/kg) and moderate (42.9 mg/kg) sites relative to the poor (7.04 mg/kg) sites. Total concentrations of Ca were highest at the rich sites (13 mg/g) compared to the moderate (5.73 mg/g) and poor (5.89 mg/g). Total Mg concentrations were higher at the rich (27.3 mg/g) than the moderate (9.47 mg/g) and poor (3.07 mg/g) sites. Using τ values throughout the soil profile compared to the parent material, we found that all three forests were moderate to weakly depleted in Ca, Mg, and K in the upper 30 cm, but P was slightly enriched due to biological uplift. Additionally, we found that calculated field nutrient release rates did not significantly differ among forest nutrient status ($p > 0.05$), indicating the limited effects from across parent materials. We also conducted a follow up batch reactor experiment at varying pH conditions (4, 5, 6) with organic acids (NaCl, catechol, and citric acid). As expected, pH 4 had the highest Mg release rate (2.19 mg/m^2/day) compared to pH 5 (1.27 mg/m^2/day), and pH 6 (0.888 mg/m^2/day), but surprisingly no effect on Ca release rates, suggesting the more acidic soils of the base cation poor soils results in higher release rates. Our results highlight the dominant contributions of parent material mineralogy has on Ca and Mg release rates, but also that weathering of primary minerals can sustain forest ecosystem productivity.

1. Introduction

The sustainability of forest harvesting in many regions, including northern New England USA, relies on the nature and abundance of soil minerals as primary factors influencing site nutrient richness (Oursin et al., 2023). Soil mineralogy is key to nutrient sustainability as timber harvesting causes the direct removal of nutrients within woody biomass and also increases the export of nutrients from the soil causing decreases in the nutrient richness of the site (Augusto et al., 2015; Garrett et al., 2021; Hornbeck et al., 1990) The removal of nutrients with whole-tree biomass has been found to decrease site fertility and forest productivity (i.e. tree growth; Cleavitt et al., 2018; Morris et al., 2014; Richard et al., 2022; Richardson et al., 2017; Roy et al., 2021; Walmsley et al., 2009). More specifically, one study across three biomes (subtropical, temperate, and boreal) found that intensive management practices such as whole-tree harvest significantly decreased tree height, diameter, and biomass as well as soil calcium (Ca) concentrations (Achat et al., 2015). Inorganic nutrients (Ca, Mg, K, P, Fe) in soils are vital for plant growth and development. Calcium supports cell development (White and Broadley, 2003), Mg regulates energy storage and photosynthesis (Wang et al., 2020), potassium (K) is involved in driving stomatal pore opening and closing (Kaiser, 1982), and phosphorus (P) is

* Corresponding author.
E-mail address: utw7wd@virginia.edu (A.M. Rice).
[1] Previous address: Department of Environmental, Geographic, and Climates Sciences, University of Massachusetts Amherst, Amherst, MA, USA

https://doi.org/10.1016/j.geoderma.2024.117081
Received 12 May 2024; Received in revised form 16 October 2024; Accepted 18 October 2024
0016-7061/© 2024 The Author(s). Published by Elsevier B.V. This is an open access article under the CC BY-NC license (http://creativecommons.org/licenses/by-nc/4.0/).

essential for forming genetic, structural, and regulatory molecules (Schachtman et al., 1998). Additionally, iron (Fe) is important in the synthesis of chlorophyll as well as maintaining the function of the chloroplast (Rout and Sahoo, 2015). While not a direct plant essential element, aluminum (Al) in soil does influence the availability of essential nutrients by binding with them especially at low pH (Bojórquez-Quintal et al., 2017). The depletion of soil inorganic nutrients is expedited as whole tree harvesting frequency increases because nutrients cannot be replenished via mineral weathering within that short period of time (Vadeboncoeur et al., 2014). Nevertheless, there is a limited understanding of differences in rates of weathering across diverse forest sites to inform sustainable harvesting guidelines.

Soil parent material is an integral aspect of site index productivity as it governs many aspects from forest species composition (Coile, 1952; Van Breemen et al., 1997), growth rates (St. Clair et al., 2008), and hydrologic dynamics (Adams et al., 2019). In northern New England, parent materials are commonly granitic and metamorphic rocks (e.g. mica schists, greenschist, phyllite) from the Taconic and Alleghanian orogenies. The primary Ca and Mg bearing minerals in granitic and metamorphic rocks include calcite, hydrothermally altered carbonates, plagioclase, chlorite and mica. Additionally, K is primarily sourced from K-orthoclase and P from apatite (Nezat et al., 2004). Therefore, soils rich in aluminosilicate minerals such as K-orthoclase, plagioclase and micas will have lower nutrient concentrations than soils with diverse mineral compositions, especially in Mg and Fe. It is worth noting that dissolution rates of silicate minerals are orders of magnitude lower than those of apatite and carbonates (Heřmanská et al., 2022; Velbel, 1993).

Soil inorganic nutrients are replenished from a combination of aboveground inputs and mineral weathering processes within the soil profile. Despite the importance of aboveground inputs in contributing to soil nutrients, the main contributor to soil nutrient richness is mineral weathering and precipitation (Jenny, 1941; Kelly et al., 1998). The rate of mineral weathering is dependent upon climate conditions, such as precipitation and temperature, and mineral composition within the soil profile, which collectively govern dissolution rates. The stability of minerals is well known, with minerals that were formed under high temperatures and pressures exhibiting greater susceptibility to weathering compared to minerals formed under lower temperatures and pressures (Goldich, 1938; April and Newton, 1992). The dissolution of minerals and their abundances directly regulate the availability of cations and buffering capacity of the soil (Manning, 2022).

Soil parent material also controls the retention and availability of base cations in forest soils through inheritance and formation of clay minerals, organic matter, and pH buffering minerals. Both clay particles and organic matter feature negatively charged surface sites that adsorb base and acid cations which contributes to the soil's capacity to retain plant essential nutrients, therefore enhancing overall soil fertility (McKenzie et al., 2004). Additionally, the negatively charged sites act as exchange sites for base cations into soil solution, making them available for uptake by plants. The availability of these nutrients is dependent on soil acidity, as increased soil acidity lowers the exchange sites occupied by base cations, which increases the solubility of these nutrients (Kaupenjohann et al., 1989). In acidic soils, acidity ($H+$) occupies sorption sites, leading to an increased leaching of nutrients from the soil (Federer and Hornbeck, 1985; Jackson and Thomas Meetei, 2018). Carbonate minerals, such as calcite, play a role in buffering soil pH as their dissolution via carbonation consumes soil protons contributing to partially neutralize soil pH (Dijkstra et al., 2003). Therefore, soil with a high buffering capacity resists changes in soil pH, promoting the availability of essential nutrients to plants.

Studies on mineral and rock weathering have employed various approaches, including modeling (Casetou-Gustafson et al., 2019; White and Brantley, 2003) and in-laboratory batch reactor experiments (Goyne et al., 2006; Richardson and Zuñiga, 2021; Velbel, 1993; Zhang et al., 2019). A comprehensive study examining the dissolution of various minerals, particularly apatite and aluminosilicates, found that apatite was the primary mineral weathered with 1 M HNO_3 in granitic-derived parent material (Nezat et al., 2007). Nazet et al. (2007) also indicated that carbonate minerals from soils derived from carbonate rocks were weathered with 1 M HNO_3, suggesting that apatite and carbonate minerals weather more rapidly and readily than aluminosilicate minerals. Therefore, the more soluble minerals will be depleted faster than aluminosilicate minerals, leading to nutrient depletion in the upper mineral soils compared to the parent material. Understanding the extent to which the soils are depleted in inorganic nutrients provides a baseline for determining the sustainability of forest management practices.

While other studies have assessed the roles of parent material on soil organic carbon (Pichler et al., 2021), physicochemical properties along a forest productivity gradient (Barnes et al., 2018), and modeled nutrient losses across various harvesting methods (Achat et al., 2018), our study is the one of the first to assess the impact of glacial till parent material, and soil solution chemistry on soil total and available nutrients along a naturally occurring nutrient richness gradient. The overarching goal of the study was to use a nutrient richness gradient to evaluate how parent material mineralogy influences soil nutrient abundance and release. For our first objective, we examined if nutrient rich (e.g. Ca and Mg) parent materials generated soils with greater exchangeable and total nutrients. We hypothesized that the soil of nutrient rich sites would have greater exchangeable and total Ca, K, Mg, and P concentrations because of the high abundance of phyllite and their physicochemical properties promoting nutrient retention. The exchangeable pools are nutrients that are readily available for plant uptake, whereas total nutrients are important for determining longer scale nutrient sustainability of a site. For our second objective, we determined if the enrichment or depletion of soil nutrients throughout the soil profile was influenced by forest nutrient richness. We calculated mass transfer (τ) values and hypothesized that these values would show either more soluble minerals at the rich site and greater depletion of Ca, K, and Mg or that there would be a greater depletion at the nutrient poor site due to the loss of low abundance minerals bearing these nutrients. Further, we hypothesized that the site with lower pH and greater DOC, which promote chemical weathering, would show a greater depletion of nutrients. For our third objective, we tested if parent material and solution chemistry affected nutrient release rates. To meet this objective, we compared dissolution rates with in-situ forest soil leachate and utilized batch reactors across the nutrient-richness gradient. We hypothesized that in-field and batch reactor Ca, K, Mg release rates would be greatest at the nutrient rich site in agreement with solution chemistry composition (e.g. pH).

2. Methodology

2.1. Study areas

2.1.1. Regional characteristics

For this study, we utilized three managed U.S. New England forests with a documented harvest history: Bartlett Experimental Forest in Bartlett, NH, Second College Grant in Coos County, NH, and Clement Woodlot near Corinth, VT (Table 1). Overall, the soils are poorly to somewhat excessively drained Spodosols and Inceptisols derived from glacial till. Through the use of Zr/Ti ratios, soil profiles were determined to be derived from uniform parent materials as coefficients of variation within forest nutrient richness were less than 30 % (Marsan et al., 1988; Supplemental Table 1).

In each forest, five circular plots 22.6 m in diameter were established within three developmental stages for a total of 15 plots per forest. This plot area was specifically chosen so that our results can be used in conjunction with or compared to long-term studies in the region (Rogers et al., 2021). The plot developmental stage (young, intermediate, or mature) was determined by the species composition, tree diameter and time since last recorded harvest. The dominant overstory vegetation is American beech (*Fagus grandifolia*), sugar maple (*Acer saccharum*), and yellow birch (*Betula alleghaniensis*) in mature forest plots. The

Table 1
Site characteristics for each of the three forests used in this study. Soil texture is the dominant texture classification at 30 to 40 cm below the surface of the mineral soil.

Forest	Nutrient Richness Level‡	Lat.	Long.	Mean elevation (a.s.l.)	Mean Annual Temp. (°C)	Mean Annual Precip. (mm)	Bedrock Geology[a]	Soil Texture
Bartlett Experimental Forest	Poor	44.048	−71.272	408	6.6	1300	Granite[a]	Sandy loam
Second College Grant	Moderate	44.887	−71.130	550	3.2	1180	Metapelite containing feldspathic metatuff, and quartz[a]	Loam
Clement Woodlot	Rich	44.049	−72.311	398	5.3	1100	Carbonaceous phyllite and limestone[b]	Sandy loam

‡ Nutrient richness is based upon Ca and Mg concentrations within bedrock.
[a] Bennett et al., 2006. Bedrock Geologic Map of New Hampshire.
[b] Ratcliffe et al., 2011. Bedrock Geologic Map of Vermont.

intermediate plots were partially defined by the additional presence of red maple (*Acer rubrum*), and white ash (*Fraxinus americana*). The presence and prevalence of pin cherry (*Prunus pensylvanica*) and striped maple (*Acer pensylvanicum*) helped define the young forest plots.

2.1.2. Natural soil Ca-Mg richness gradient

These three forests represent a natural soil Ca-Mg gradient with Clement Woodlot as the "Rich" site, Second College Grant as the "Moderate" site and Bartlett Experimental Forest as the Ca "Poor" site. This gradient is due to the range in parent material composition (Ratcliffe et al., 2011). Because this region of the US was glaciated until quite recently (ca. 14,000 yrs ago), the soil parent material does not directly correspond to the bedrock but reflects instead a range of neighboring materials carried by the Laurentide ice-sheet. While it is not possible to clearly pinpoint the origin of this surficial material, the direction of low and typical distances covered by the sediments in the region allows us to approximate the parent material as resulting from local bedrock extending about 1.5 km NW of the sites (Koteff and Pessl, 1981). The rich site is the most different of the three forests because of the high abundances of apatite and carbonate in the glacial till parent material. This rich site is part of the Connecticut Valley Trough, specifically the Waits River Formation with limestone and phyllite as the major lithologic constituents (Lyons et al., 1997). The limestone is dark bluish-gray in color and micaceous rich whereas the phyllite is dark to silvery gray with muscovite, biotite and quartz with occasional chlorite (U.S. Geological Survey, 2023b). Additionally, while this area is predominantly mapped as Colrain Series, a coarse-loamy, mixed, active, frigid Humic Dystrudept (Soil Survey Staff, 2023), field and laboratory measurements suggest that the sampled site is more accurately classified as an Oxyaquic Eutrudept. The moderate site, Second College Grant, is part of the Central Maine Trough, specifically the Aziscohos Formation with metapelitic schists containing coticule laminations, quartz lenses, and feldspathic metatuff as the major lithological constituents (Lyons et al., 1997; U.S. Geological Survey, 2023a). Additionally, this area is mapped predominantly as Peru Series which is a coarse-loamy, isotic, frigid Aquic Haplorthod. The poor site, Bartlett Experimental Forest, is predominantly Conway Granite which is a coarse-grained granite with a distinct pink hue. The Conway granite is composed of biotite, plagioclase, and perthic feldspar (Liese, 1973). Additionally, this area is predominantly mapped as Marlow Series which is a Coarse-loamy, isotic, frigid Oxyaquic Haplorthod.

2.2. Field sampling

One soil pit (~0.5 m wide) was excavated per plot within each of the three forests for a total of 45 soil pits (Supplemental Fig. 1). The pits were dug to expose a new, unaltered face for sampling and size varied due to physical restrictions from roots and rocks. The pits were dug to a depth of 1 m, or until a restrictive layer such as a fragipan was encountered. The deepest soils were found at the Ca rich site, with 14 out of the 15 pits reaching a depth of 90 cm or more below the surface of the mineral soil. Additionally, a soil bulk density sample was taken at the top of the mineral soil and ~ 50 cm deep for two samples per pit using a metal soil corer 7.30 cm in diameter and 10.8 cm long.

Soil samples were collected in 5 cm increments from the surface to 30 cm depth and in 10 cm increments from 30 cm to the base of the soil pit. A core was used to sample the underlying parent material or confining layer. A total of 621 soil samples were collected across the 45 plots. This sampling strategy aimed to capture intra-horizon variability and identify depth-related changes in physicochemical properties, which may be obscured by horizon-based sampling. Depth specific sampling also enables us to use this data in a forest nutrient cycling model (Orton et al., 2016; Sulieman et al., 2018).

Additionally, zero tension lysimeters were installed 50 cm below and parallel to the top of the mineral soil to collect soil water (Jordan, 1968). The lysimeters are 348 cm^2 and drain into a 2 L bottle buried at the bottom of each soil pit. Each spring and fall water was collected from the bottles for elemental analyses and a subsample was frozen for dissolved organic carbon analyses.

2.3. Sample processing and inorganic nutrient analysis

2.3.1. Parent material mineral abundance

One representative soil sample collected at a depth of 30 cm from each of the three forest sites was selected for in-depth Electron Probe Micro Analysis (EPMA). Samples were prepared commercially by Mineral Optics Laboratory (Wilder, VT) where approximately 5 g of sample was impregnated with epoxy and polished to submicron levels suitable for hyperspectral mapping. Epoxy resin samples were then analyzed using Cameca SX-Five-Tactis electron microprobe located in the University of Massachusetts Amherst Department of Earth, Geographic, and Climate Sciences (Amherst, MA). Five elements (Na, Fe, Ca, Al, Si) were mapped using Kα fluorescence on dedicated wavelength-dispersive spectrometer (WDS) detectors and five elements (Mg, P, K, Ti, Mn) using Kα fluorescence on two electron-dispersive spectrometer (EDS) channels. Column conditions were set at 15 keV, 249nA and dwell time set at 0.02 s.

2.3.2. Physical processing and characteristics

Mineral soil samples were air dried, passed through a 2 mm sieve and a subsample of the < 2 mm fraction was homogenized using a mortar and pestle. Physical characteristics were determined using the homogenized < 2 mm fraction for analyses of texture, pH, and organic matter content. Particle size distribution of sand (< 2 mm to 63 μm), silt (63 μm to 2 μm), and clay (< 2 μm) was analyzed following Bouyoucos hydrometer method (Gee and Bauder, 1986) where the fraction of each particle size was recorded by mass.

For soil pH, 10 g of 0.01 M $CaCl_2$ was added to about 4 g of soil and shaken for at least 12 h. Once settled, the pH of the supernatant was measured using a Fisher Scientific pH meter. Soil organic matter (%) was

estimated through loss-on-ignition (LOI) by combusting ~ 5 g of soil at 550 °C for at least 12 h. Every 30 samples included a standard reference material and a blank.

For soil dissolved organic carbon, soil water samples were filtered to < 0.45 μm and acidified to a pH 2 with 10.2 M HCl. Non-particulate dissolved organic carbon was measured using a TOC-L series Shimadzu total carbon analyzer with blanks below detection limits and variability within 2 %.

2.3.3. Exchangeable soil nutrients

To quantify the exchangeable inorganic nutrients in mineral soils, we followed a modified version of an established extraction procedure (Tessier et al., 1979). In this procedure, 2.0 g of < 2 mm soil were extracted using 30 mL of 0.1 M NH_4Cl and shaken for 24 hrs. The soil slurry was then centrifuged at 2800 rpm for 1 h and filtered to < 0.45 μm. The resulting solution was acidified to 2 % HNO_3 to prevent microbial and fungal activity until analyzed.

2.3.4. Total soil nutrients

A total digestion of the mineral soil followed a modified version of USEPA Method 3052. Prior to digestion, samples with 8 % or higher organic matter underwent combustion at 550 ℃ to remove organic carbon. To achieve total digestion, 20 mg of sample was placed in a 30 mL perfluoroalkoxy alkane (PFA) vial, along with 2.5 mL of 15.6 M HNO_3 and 2.5 mL of 28.9 M HF. The vials were heated at 170 ℃ for 48 hrs. After 48 hrs, the mixture was dried down to a moist paste, resuspended with 2 mL of 15.6 M HNO_3, and dried down again. This process was repeated once more before the final paste was resuspended in 5 mL of 7.8 M HNO_3 and heated at 170 ℃ for 48 hrs. The solution was then diluted to 50 mL using 18.2 MΩ•cm deionized water. A procedure blank, along with two standard reference materials were included with every 25 samples.

2.3.5. Elemental concentration analysis

Concentrations of macroelements and nutrients (Al, Fe, Ca, K, Na, Mg, Si, P) in soil exchangeable, total, soil solution, and batch reactor samples were determined using an Agilent 5110 Inductively Coupled Plasma-Optical Emissions Spectrometer (ICP-OES; Agilent, Santa Clara, CA, USA). A nine-point multi-element standard curve was used for calibration. To ensure measurement accuracy, a Standard Reference Material (NIST 2709a San Joaquin Soil) and an in-house Bs horizon soil standard were analyzed every 25 samples. Measured recovery rates for the San Joaquin soil were within 80–11 % of certified values, and in-house Bs concentrations only varied 1–25 % of the average in-house value. Elemental concentrations in the blanks were below 0.01 mg/L for all elements analyzed.

2.4. Batch reactors for weathering rates

We conducted a batch reactor experiment to determine how mineral release rates may be influenced by pH among the dominant rock types within each nutrient richness. In this laboratory experiment, 3.00 (± 0.01) g of each soil sample from the depth ranges 5 to 10 cm, 30 to 40 cm, and the parent material were immersed in a 40 mL solution composed of 0.01 M NaCl, 0.01 M catechol, and 0.01 M citric acid. The pH of the solutions was adjusted to 4, 5, or 6 using concentrated trace metal grade HCl and NaOH, since the pH of the field soil solution varied from 4.8 to 6.7 among the three forest nutrient richness levels. The samples were shaken for two-week intervals for a total of 10 weeks. After shaking, the solutions were centrifuged at 2600 rpm for 1 hr, supernatant was decanted, and a new solution of the same pH was added. A new solution was added after every two weeks to avoid precipitation and oversaturation of elements in solution, to provide discretized replication for the time series and to provide adequate sample mass for elemental analyses. The pH of the supernatant was measured to determine changes in pH following the 2 weeks of weathering. The supernatant was then acidified with HNO_3 for stability and a subsample aliquot was diluted for elemental analyses using the same ICP-OES procedure as the soil and rock nutrients.

To calculate release rates of the elements, surface area was measured. Soil surface area for two depths from each forest nutrient richness was analyzed using the Brunauer-Emmett-Teller method by the particle technology labs (https://particletechlabs.com/).

2.5. Data processing

2.5.1. Parent material mineral abundance

Three areas were mapped on each prepared sample using decreasing beam sizes of 20, 10 and 5 μm. The resulting data were plotted for graphical representation and multivariate analysis at all resolutions. At the finest resolution (5 μm), single pixel data were subjected to hierarchical clustering analysis using JMP® Pro. Characteristic groupings of elemental relative intensity ratios were used to identify specific minerals within the various clusters, including pixels representing void space. A large portion of each sample consisted of pixels characteristic of phase overlaps or 'edges', where two or more minerals contributed to the signal and could not be definitively identified. Following mineral identification, we calculated mineral coverage of the map area (μm^2) based on the size of the pixel (25 μm^2), excluding void space. Quantification error for individual mineral groups was determined to be linearly correlated to the area covered by "edges" so that the total error was distributed with equal weight across the various mineral area fractions.

2.5.2. Field: Soil nutrients and base saturation

Exchangeable and total soil nutrient concentrations were standardized to elemental mass per mass of soil using the amount of soil used for each sample. The cation exchange capacity (CEC) was estimated by summing the milliequivalents (meq) of exchangeable cations including Al, Fe, Ca, Mg, K, and Na. Base saturation (%) was then calculated by taking the sum of the base cation (Ca, Mg, K, Na) concentration divided by each elements charge and dividing by the CEC.

2.5.3. Field: Soil to solution nutrient release rates calculation

Elemental concentrations of the soil solution were used to estimate the in-field nutrient release rates of soil among the nutrient-richness gradient. Estimates of soil nutrient release rates ($g/cm^2/yr$) were calculated using the following formula:

$$\text{Soil nutrient release} = \frac{SS}{Bd*Depth*LA*SA} \quad (1)$$

where *SS* is the elemental concentration leaching rate (g/yr), *Bd* is the bulk density of the soil from the profile (g/cm^3), *Depth* is the depth (cm) of soil from the top of the mineral soil to the top of the lysimeter, *LA* is the area of the lysimeter that is collecting soil water (cm^2), *SA* is the average surface area of the soil (cm^2/g). Soil nutrient release rates were calculated for each plot within each soil nutrient richness (n = 45).

2.5.4. Soil chemical index of alteration

Since feldspars are a major component of rocks and soil, determining the changes in chemical composition associated with feldspar weathering provides insight to the extent of weathering the soil has undergone. The chemical index of alteration was used to determine the relative degree of weathering throughout the soil profile (Nesbitt and Young, 1982):

$$\text{Chemical Index of Alteration} = \frac{Al_2O_3}{(Al_2O_3 + Na_2O + CaO + K_2O)} \quad (2)$$

where molar values for each oxide were calculated from total digest cation concentrations. The assumption in this calculation is that all the Ca at these sites is in CaO.

2.5.5. Soil base depletion index

In addition to the chemical index of alteration, we calculated the base depletion index to determine the ratio of oxides of base cations compared to oxides that comprise clay and secondary minerals in soils. We used the following equation to calculate the base depletion index (Anda et al., 2023; Jien et al., 2016):

$$\text{Base Depletion Index} = \frac{(CaO + MgO + Na_2O + K_2O)}{(Fe_2O_3 + Al_2O_3 + TiO_{2)}} \quad (3)$$

where molar values for each oxide were calculated from total digest cation concentrations. The assumption in this calculation is that all the Ca at these sites is in CaO.

2.5.6. Soil tau profile plots

A mass transfer coefficient (τ) was calculated throughout the soil profile for each inorganic element to determine the depletion or enrichment of elements relative to the parent material (Brimhall and Dietrich, 1986) using the following equation adapted from Wacket et al. (2018):

$$\tau_{\text{j,soil}} = \frac{C_{j,soil} * C_{Ti,\,pm}}{C_{j,pm} * C_{Ti,soil}} - 1 \quad (4)$$

where the element of interest (*j*) in the weathered soil (*soil*) or parent material (*pm*) were normalized to Ti (*Ti*), an immobile element. Concentrations (C) for the *soil* were used for each depth within each plot among nutrient richness. Concentrations for the *pm* were the *j* and *Ti* concentration of the deepest depth horizon sampled for each plot among the nutrient richness gradient. Tau was calculated for each depth within each plot among the nutrient richness gradient. A positive τ value represents an enrichment of a target element in the soil compared to the parent material, whereas a negative τ value represents a depletion (e.g. Bonar et al., 2023; Brantley and Lebedeva, 2011; Richardson and King, 2018).

2.6. Statistical analyses

To address the assumption of normality, the physicochemical variable, and all exchangeable nutrient and total Ca, K, and Mg concentrations were log-transformed prior to analysis. A multivariate mixed-effects analysis of variance (MANOVA) was used to investigate the influence of soil physicochemical characteristics (i.e. clay content, organic matter, pH) on exchangeable and total nutrient concentrations.

To assess the impact of nutrient richness and depth on soil nutrient concentrations and physical characteristics, we used two-way MANOVA. Nutrient richness and depth were treated as categorical fixed effects, while nutrient concentrations served as the response variable. To ensure independence, each plot (n = 15) within each nutrient richness was considered an independent sampling unit and modeled as a random effect.

Weathering indices (i.e. soil nutrient release rates, chemical index of alteration, base depletion index), tau plots, and soil solution elements were analyzed using mixed-effects ANOVAs to determine differences among forest nutrient richness and depth. Nutrient richness and depth were treated as categorical fixed effects while solution concentration, weathering indices and tau values served as response variables. Again, each plot was modeled as a random effect to ensure independence. No transformation was needed for these analyses to meet the assumption of normality.

Elemental concentrations in soil solutions were analyzed using ANOVA to determine differences among forest nutrient richness. All elements were log-transformed to meet the assumption of normality prior to analyses. Also, soil nutrient release rates were analyzed using ANOVAs to determine differences among forest nutrient richness and the influence of soil physicochemical characteristics. Tukey's Honest Significant Difference (HSD) tests were used to identify pairwise differences within factors exhibiting statistically significant overall effects.

For the soil weathering experiment, an ANOVA was conducted to determine the influence of forest nutrient richness, pH, and depth on nutrient release rates. A logarithmic transformation was used on Al, Ca, Mg, and P concentrations to meet the normality of residuals assumption.

All statistical analyses were performed using *R* version 4.2.3 (R Core Team, 2023).

3. Results and discussion

3.1. Soil properties across nutrient richness gradient

Forest soil characteristics including clay content, soil organic matter, pH, and base saturation play critical roles in nutrient sorption and retention within the ecosystem. Examining the physicochemical properties along the nutrient richness gradient as part of our first objective, we observed significant differences in soil organic matter, pH, and base saturation, but not clay content (Fig. 1; Supplemental Table 2). We found that clay content was not influenced by nutrient richness ($p = 0.71$) even though the moderate sites had a higher clay content (15.3 %), than the rich (7.34 %) and poor (9.06 %). Although not significant, this observation agrees with previous studies on young granitic soils having low clay content such as at the poor site and young micaceous and schists having high clay content such as at the rich site (Righi and Meunier, 1991). Clay content did not change with depth across the nutrient gradient ($p = 0.15$), indicating that pedogenesis has not formed strongly contrasting horizons across the varying soil materials.

Soil organic matter content decreased significantly with depth, which was expected due to diminished biological inputs in deeper soil horizons ($p < 0.01$; Fig. 1). Overall, soil organic matter differed among forest nutrient richness ($p < 0.01$). Moderate sites exhibited the highest organic matter content (6.73 %), followed by poor sites (6.66 %), and rich sites having the lowest (6.02 %). This pattern aligns with expectations, as higher clay content, although not significantly different between sites, can enhance organic matter retention through increased mineral protection and surface area sorption (Paul, 2016). This trend was consistent across all nutrient richness levels, with rich sites consistently displaying lower clay and organic matter content.

Despite pH being significantly higher at the rich sites ($p < 0.01$; Fig. 1) than the poor and moderate sites, the measured pH values of 4.92 would be considered strongly acidic, which decreases even further at the moderate site with pH 4.27 and poor site with pH 4.11. This range in pH values are similar to other studies in the region that report pH ranging from about 3 to 7 (Armfield et al., 2019; Hazlett et al., 2020; Schattman et al., 2023). The acidity of the soil is likely attributed to a combination of soil mineralogy and calcium content. The weathering of aluminosilicate minerals increases the acidity (decreases pH) of the soil while the parent material containing calcium (i.e limestone) is a buffering agent, resisting changes in pH. The calcium content of the soil over time many have been affected by factors such as acid rain, diminishing the buffering capacity of the soil and allowing the mineral weathering and organic matter decomposition to have a greater impact on soil pH. Additionally, the observed increase in pH with depth ($p < 0.01$) is likely attributed to the input of organic acids from decomposition of organic matter in the surface horizons, which can contribute to acidification.

Similar to pH, base saturation varied significantly along the forest nutrient richness gradient ($p < 0.01$), with rich sites exhibiting the highest values (54.4 %), followed by moderate (19.6 %) and poor (4.79 %). At the rich site, base saturation increased with depth ($p < 0.01$), mirroring the depth-dependent pattern observed in pH. Soil pH and mineralogy directly influence base saturation by affecting the availability of cation exchange sites and the types and abundance of clay minerals. The observed base saturation values in these forests are comparable to those reported in other regional studies (5–25 %; Hazlett et al., 2020). Base saturation levels below 15 % has been linked to

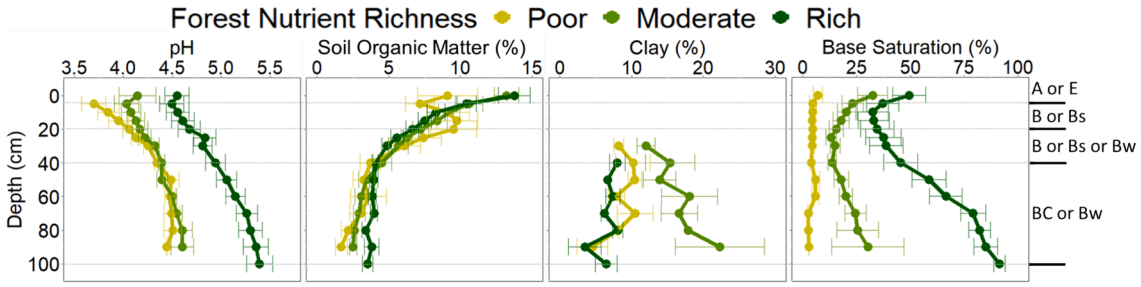

Fig. 1. The average soil clay content, soil organic matter, pH, and base saturation through the soil profile spanning a nutrient richness gradient. The estimated soil horizons for the sites are delineated by a dashed gray line on the right. Each point represents the mean with error bars indicating the standard error.

inhibited tree growth (Cronan and Grigal, 1995; Walthert et al., 2013), suggesting potential growth restrictions in nutrient poor and moderate sites. These results support our initial hypothesis and objective, indicating that despite similar climate and vegetation, the soil parent material has generated lasting effects on the soil acidity and nutrient status. This underscores the importance of considering site-specific nutrient conditions for sustainable management.

3.2. Soil nutrients across nutrient richness gradient

3.2.1. Parent material mineral abundance

Mapping by EPMA of the major soil elements revealed differences in the texture and general mineral composition of the soils across sites. The soil of the poor site appeared to be dominated by sand-size Si, Na, and Al rich phases embedded in a matrix of fine sand (Fig. 2; Supplemental Figs. 1 and 2). The moderate site was dominated by aggregates of Al-rich elongated minerals (i.e. micas) with small Si-rich and Na rich phases (Fig. 2). The presence of a typical garnet porphyroblast in the sample is notable, and points to the metamorphic nature of the parent material at the moderate site. The rich site was dominated by micrometric Si-rich minerals with smaller Na, Al and Mg rich phases and few sub-micrometric minerals (Fig. 2).

To further characterize the parent material mineralogy, we identified and quantified the mineral phases in the parent material from each forest to provide a baseline for future nutrient availability (Table 2). Quantitative analysis by EPMA confirms that the soils from all sites were dominated by quartz and plagioclase. For Ca-bearing minerals in all sites, Ca was principally present in plagioclase and apatite with the poor site exhibiting the lowest total abundance in these minerals (4.8 %). Interestingly, there was no clear mineralogical trend that follows the site nutrient richness index. However, it appears that the nutrient bearing minerals varied across the gradient, with Na and K in feldspars in the poor site, fine clay minerals in the moderate site, and large amphiboles in the rich site. These results partially support our hypothesis for objective 1, as we did not observe a clear difference in the total amount of nutrient bearing minerals across the site. However, each site showed specific characteristics such as different grain sizes and different dominant nutrient-bearing mineral types.

3.2.2. Total concentrations of soil elements

We investigated if the total nutrient concentrations of soil provide information on the overall edaphic nature of a site and is a strong indicator of the long-term sustainability of the soil fertility for multiple harvests as part of our first objective. Overall, total elemental concentrations aside from P varied significantly along the forest Ca-Mg nutrient richness gradient ($p < 0.01$; Fig. 3; Supplemental Table 3). Total Ca concentrations were highest ($p < 0.01$) at rich sites (13.0 mg/g) compared to the moderate (5.73 mg/g) and poor (5.89 mg/g) sites and concentrations increased with depth ($p < 0.01$). The soil total Ca concentrations in these forests were similar to other studies in the region, that ranged from 2.5 to 24 mg/g (Dijkstra and Smits, 2002; Finzi et al., 1998; Richardson and Friedland, 2016). This large range is attributed to differences in parent material compositions. The total soil Ca concentrations across the nutrient richness gradient is attributed to plagioclase mineral abundance in the parent material, also found by other studies in the region (Bower et al., 2023; Likens et al., 1998; Table 2). Total Mg followed a similar trend where the rich site was significantly ($p < 0.01$) higher (27.3 mg/g) than the moderate (9.47 mg/g) and poor (3.07 mg/g) and increased with depth ($p < 0.01$). These sites fall within the natural total Mg concentration range in this region (2 mg/g to 168 mg/g; Woodruff et al., 2015), and the Mg concentrations correspond to amphibole abundance (Eberl and Smith, 2009; Fig. 2; Table 2). The total Ca and Mg concentrations highlight the natural nutrient richness gradient of the studied forests, supporting that parent material mineralogy does control nutrient soil nutrient concentrations.

We expected the total soil K concentrations to be inverse to the Ca and Mg concentration trends as their host aluminosilicate minerals (e.g. K- feldspar, and micas) vary with lithologic formation (Safonov et al., 2011) and our results support this hypothesis. We found that total K concentrations were significantly higher ($p < 0.01$) at the poor site (28.8 mg/g) and lower at the moderate (10.8 mg/g) and rich (6.05 mg/g) sites. There were no significant differences in K concentrations with depth ($p = 0.32$). These total K concentrations fall within the observed range (4.2 mg/g to 51 mg/g; Woodruff et al., 2015) for this region. Total soil K concentrations strongly corresponded to parent material K-feldspar, and mica abundance (Fig. 3; Table 2; Eberl and Smith, 2009). Unlike Ca and Mg, which are more mobile due to their presence in weathering susceptible minerals like plagioclase and amphiboles, K is less likely to be mobilized due to the greater resistance of micas to weathering.

Total P concentrations did not significantly vary among forest nutrient richness levels ($p = 0.75$), with moderate (1.29 mg/g) and rich sites (1.23 mg/g) exhibiting slightly higher P concentrations than poor sites (1.17 mg/g). Although these values are lower than those reported in other regional studies (5–27 mg/g; Woodruff et al., 2015), they are comparable. While apatite was detected in trace amounts across all sites using EPMA, they were detected in trace amounts, contributing to the overall lower P content of these soils compared to previous studies.

Total Al concentrations varied significantly among the forest nutrient richness gradient ($p < 0.01$). The highest concentrations were observed at the moderate sites (70.1 mg/g), followed by the rich sites (64.5 mg/g) and the poor sites (56.7 mg/g). These concentrations were strongly correlated with clay content, which in these sites, is directly linked to the abundance of Al-rich minerals in the parent material (Table 2). Also, the elevated Al concentrations contribute to the acidic nature of the soils at these sites. This suggests that the weathering of aluminosilicate minerals in the soil is a primary driver of soil acidity. Total Al concentrations did not vary significantly with depth ($p = 0.48$), indicating that Al is primarily bound in recalcitrant minerals, such as clays, rather than being readily exchangeable.

Additionally, we examined the potential sorption of inorganic nutrients to secondary Fe oxyhydroxides, which we approximate with total Fe concentrations. We found that Fe varied significantly with forest nutrient richness ($p < 0.01$) with rich (33.2 mg/kg) and moderate (34.3

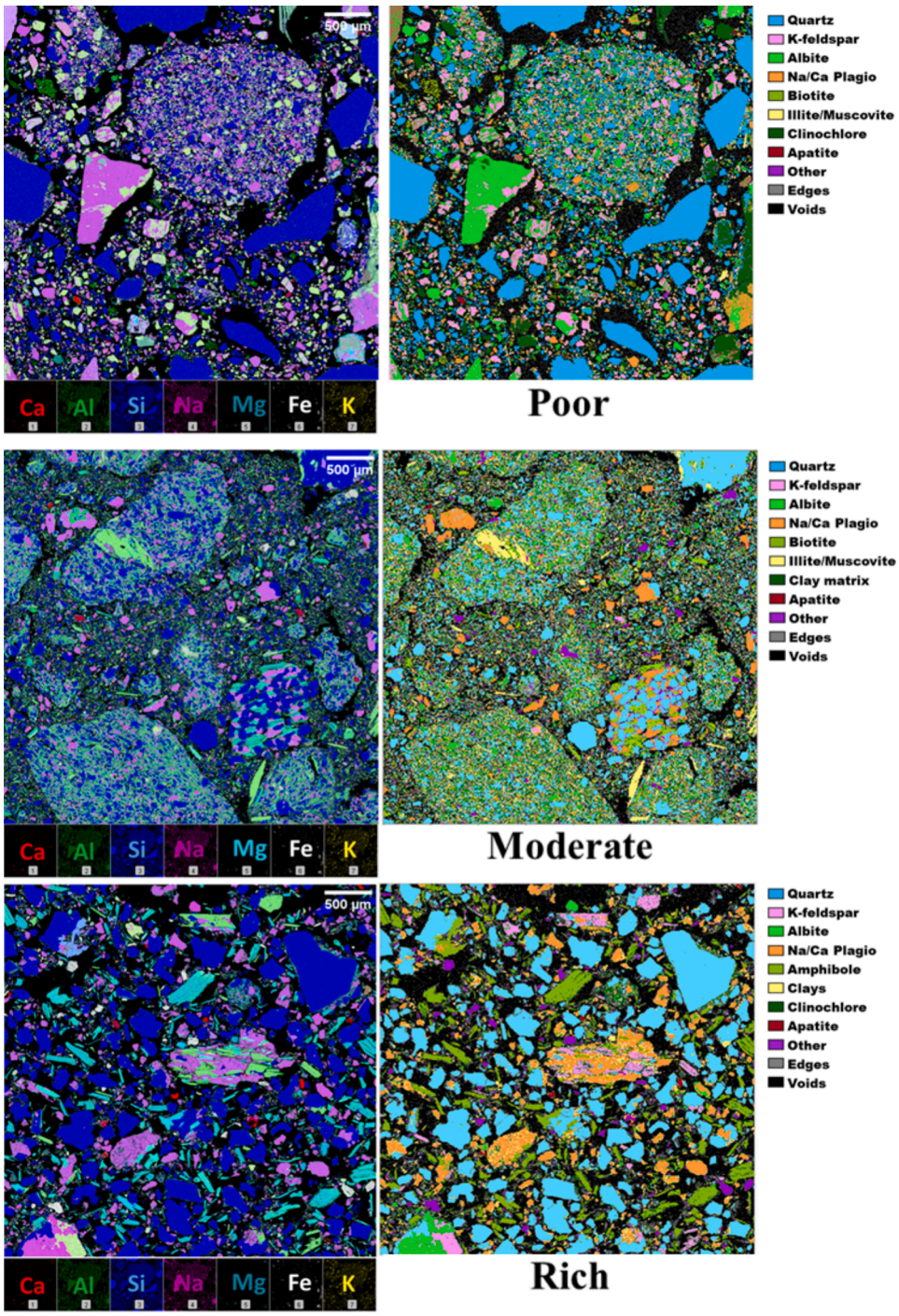

Fig. 2. Electron microprobe elemental maps of representative soils from each site and results of the clustering characterization of the maps using hierarchical agglomerative clustering. Clustering characterizations identify minerals based on relative elemental compositions.

mg/kg) sites having higher total Fe compared to poor (19.1 mg/kg). Soil total Fe concentrations are attributed to amphibole, mica, and clay mineral abundances in the soil (Fig. 3; Table 2; Eberl and Smith, 2009). Total Fe was also significantly increased with depth ($p < 0.01$) where concentrations were depleted in the E horizons, and significantly increased with depth into a diagnostic Bs horizon (spodic horizon) for the poor site. This highlights that the formation of secondary Fe oxides in the spodic horizon either did not increase sorption capacity for nutrients or that chemical weathering and sourcing of nutrients throughout the rest of the soil profile is a more dominant controlling factor (Fink et al., 2016).

3.2.3. *Exchangeable soil elements*

Exchangeable nutrients are the most readily available for tree uptake and were investigated to assess how parent material mineralogy influences their availability their influence from parent material mineralogy. We observed significant effects that followed the forest nutrient richness gradient ($p < 0.01$) with the highest average Ca concentration of at the rich site (758 mg/kg) and the lowest at the poor site (51.3 mg/kg; Fig. 4; Supplemental Table 3). The moderate sites (194 mg/kg) fell in between the other two sites. These soil concentrations are similar to other studies, where the typical range for exchangeable Ca is between 30 and 200 mg/kg, with the exception of the rich site, which was more than

Table 2
Parent material mineral abundance for each forest nutrient richness. Mineral phases were identified using electron probe microanalysis. Micas refers to the combination of muscovite, biotite, and chlorite. The error associated to each mean is based on the linear propagation of the area coverage uncertainty.

Mineral Phases	*Bulk Mineral Abundance of Parent Material (%)*		
	Poor	Moderate	Rich
Quartz	41.1 (4.8)	33.4 (7.6)	45.9 (8.0)
Ca-Plagioclase*	4.6 (0.5)	7.2 (1.6)	6.6 (1.1)
Na-Plagioclase	24.0 (2.8)	13.4 (3.0)	10.1 (1.8)
K-feldspar	13.0 (1.5)	0.2 (0.1)	4.5 (0.8)
Amphibole	6.9 (0.8)	–	14.8 (2.6)
Micas	8.5 (1.0)	18.9 (4.3)	8.3 (1.4)
Clay Minerals	1.7 (0.2)	23.3 (5.3)	6.1 (1.1)
Apatite	0.2 (0.1)	0.1 (0.1)	0.3 (0.1)
Other	0.3 (0.1)	3.4 (0.8)	3.4 (0.6)

* Ca-plagioclase comprise all plagioclase with a Ca:Na ratio over 1:4.

3x's higher than the range extent observed in non-calcareous literature (Asmare et al., 2023; Bowden et al., 2019; Dijkstra and Smits, 2002; Oursin et al., 2023). According to the NRCS and other studies, exchangeable soil Ca concentrations within this range are unlikely to be detrimental to non-woody and woody plants (Ericsson, 1994; Soil Survey Staff, 2023). However, studies have noted reduced basal area growth in sugar maple (Schaberg et al., 2006) and diminished tree height in various species (Li et al., 2023) growing on soils with exchangeable Ca values at the lower end of this range. Therefore, we expect forest productivity should not be significantly hindered in our studied forests even though they are on a natural nutrient gradient.

Similarly, exchangeable soil Mg concentrations were significantly higher in the rich (41.5 mg/kg) and moderate (42.9 mg/kg) sites compared to the poor sites (7.04 mg/kg; $p < 0.01$; Fig. 3). Mica and amphibole minerals are the main source of Mg in these soils and the exchangeable Mg concentrations correspond to the abundance of these minerals at each forest (Fig. 4; Table 2). Exchangeable Mg concentrations along the nutrient richness gradient were below the typical range (60 to 300 mg/kg) for adequate nutrient availability to support growth (Hornbeck et al., 2019). Other studies have reported Mg concentrations ranging from 11 to 266 mg/kg in forest soils which fall within this range (Oh et al., 2007; Olorunfemi et al., 2018; Schaberg et al., 2006). The study with the lowest values saw varying growth rates but these rates were attributed to the Ca and P availability since Mg availability was relatively similar among the stands they examined (Schaberg et al., 2006).

We expected that exchange K concentrations would not directly correspond with the Ca-Mg gradient, as K-bearing aluminosilicate minerals are distinct from Ca-Mg bearing ones. However, we found the exchangeable K concentrations were significantly higher in the rich (38.8 mg/kg) and moderate (35.6 mg/kg) sites compared to the nutrient poor site (18.9 mg/kg; $p < 0.01$; Fig. 3). This observed range falls within the range reported in other studies of forest soil exchangeable K (50 to 429 mg/kg; Boerner et al., 2003; Bowden et al., 2019; Olorunfemi et al., 2018). According to previous studies, exchangeable K concentrations exceeding 150 mg/kg should support productivity of both non-woody and woody plants (Ericsson 1994; Hornbeck et al., 2019).

Exchangeable P concentrations did not significantly vary among forest nutrient richness ($p = 0.07$). Although not significant, a trend was observed, with the moderate nutrient richness sites exhibited the highest concentrations (1.31 mg/kg), followed by the poor (0.735 mg/kg) and rich sites (0.570 mg/kg; Fig. 4). Despite variations in soil extraction procedures used to evaluate exchangeable P (e.g. Mehlich-3 vs Olsen vs Bray-P1), our measured concentrations are consistent with other studies that ranged from 0.8 to 4.0 mg/kg (Liu et al., 2014). Notably, Gradowski and Thomas (2006) found that forest productivity may be P-limited when exchangeable P falls below 5 mg/kg, suggesting that P availability could be a tree productivity constraint across the forest nutrient gradient. Additionally, exchangeable P concentrations can be influenced by clay content and Al concentrations. Given that total Al concentrations followed a similar pattern to exchangeable P concentrations, it is likely

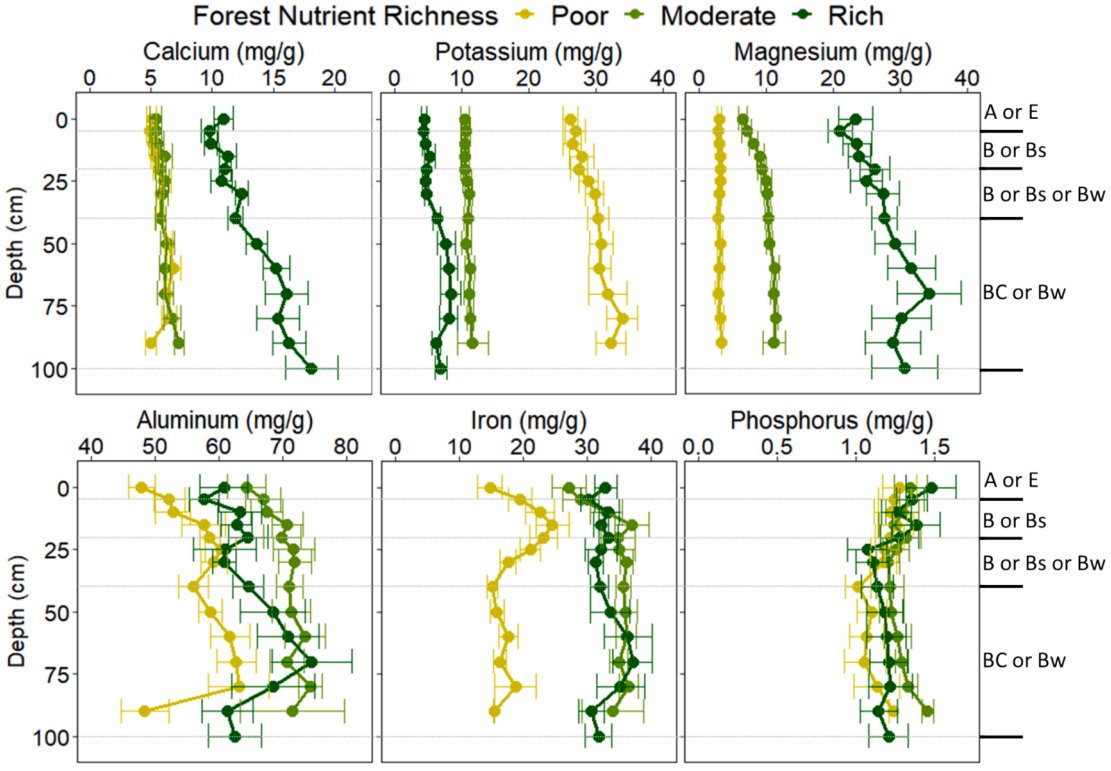

Fig. 3. Total nutrient profiles (Ca, K, Mg, Al, Fe, P) across forest nutrient richness. The y-axis corresponds to the depth below the top of the mineral soil. The estimated soil horizons for the sites are delineated by a dashed gray line on the right. Each point represents the mean with error bars indicating the standard error.

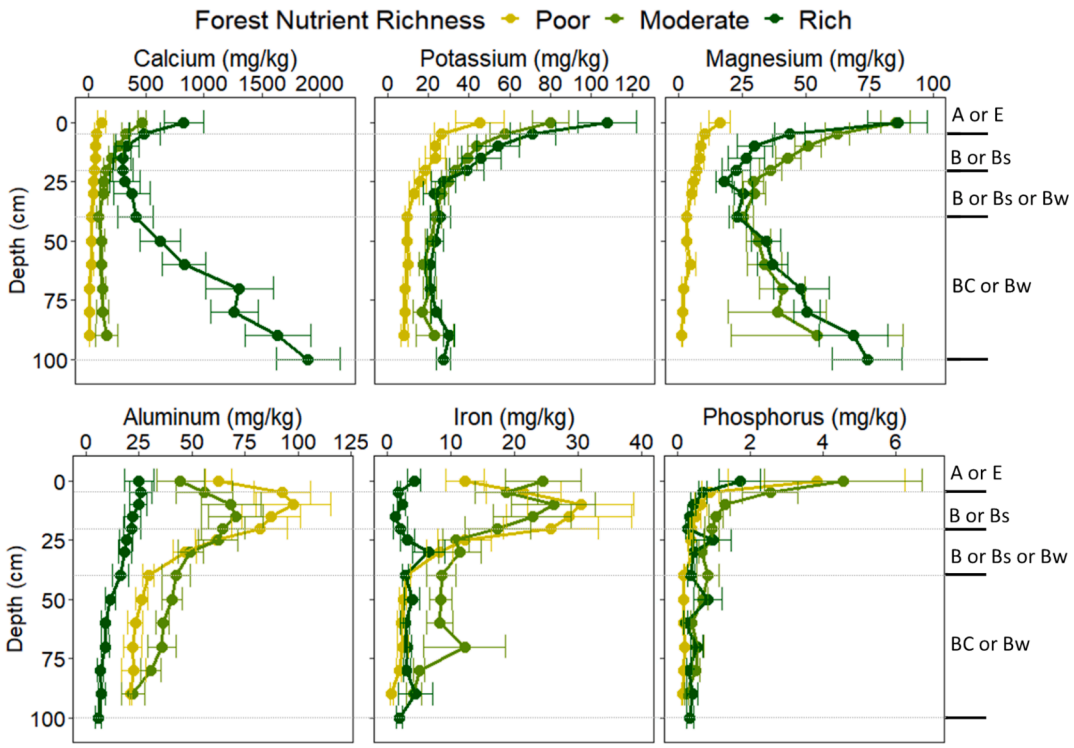

Fig. 4. Exchangeable elemental profiles (Ca, K, Mg, Al, Fe, P) across a nutrient richness gradient. The y-axis corresponds to the depth below the top of the mineral soil. The estimated soil horizons for the sites are delineated by a dashed gray line on the right Each point represents the mean with error bars indicating the standard error.

that clay content plays a more dominant role in controlling exchangeable P availability than P mineral abundance in these forests.

Exchangeable Al concentrations varied significantly among the forest nutrient richness gradient ($p < 0.01$; Fig. 4). The highest concentrations were observed at the poor sites (59.1 mg/kg), followed by the moderate sites (51.4 mg/kg) and the rich sites (16.1 mg/kg). While our measures values fall within the typical range of 10–300 mg/kg for exchangeable Al, the concentrations varied substantially among sites, likely reflecting the clay mineral abundances and their control on Al concentrations in the soil (Dragun, 1988; Álvarez et al., 2005). In contrast, exchangeable Fe did not significantly vary across the forest nutrient richness gradient ($p = 0.54$). While moderate sites had slightly higher Fe concentrations (15.1 mg/kg) compared to poor (14.1 mg/kg), the rich sites had the lowest concentrations (3.17 mg/kg). However, exchangeable Fe concentrations decreased significantly with depth ($p < 0.01$), likely due to the weathering of Fe-bearing minerals such as amphiboles and micas. As weathering progresses, Fe may be released from these minerals and transported downwards in the soil profile, leading to higher concentrations in deeper horizons and lower towards the surface.

3.2.4. *Weathering indices throughout the soil profile*

The chemical index of alteration varied significantly among forest nutrient richness levels ($p < 0.01$) and decreased significantly with depth ($p < 0.01$; Fig. 5; Supplemental Table 4). Moderate sites displayed the highest chemical index of alteration (72.7 %), followed by rich sites (68.0 %), while poor sites had the lowest (52.7 %). The higher chemical

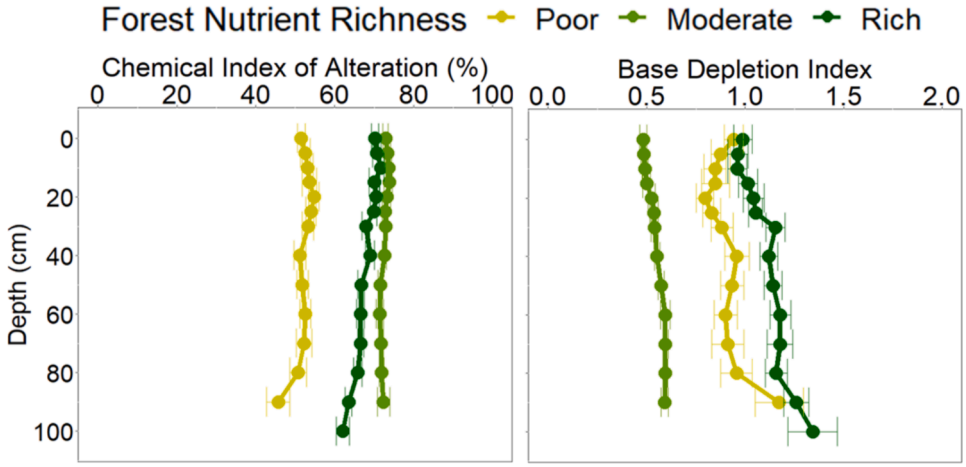

Fig. 5. Weathering indices throughout the soil profile showing the chemical index of alteration by percentage in the first panel and the base depletion index which is a unitless number in the second panel. For each index, the three nutrient richness gradient levels are shown in differing colors. Each point represents the average with standard error bars.

index of alteration percentages indicates more advanced silicate weathering, suggesting that poor sites have undergone the least silicate weathering. However, this is likely attributed to the higher abundance of Na plagioclase and K feldspar in these soils which are most present in this value range (Nesbitt and Young, 1989). The observed decrease in chemical index of alteration with depth is consistent with the expectations that upper horizons experience more weathering than deeper horizons, which are close to the parent material. The percentages in our study align with previous reports, which typically indicate lower percentages (50–60) in recently formed soils (e.g. from glaciation; Nesbitt and Young, 1982). Given the climate of these sites, moderate precipitation and temperature conditions are likely to have contributed to some degree of silicate weathering, resulting in chemical indexes of alteration slightly exceeding the typical range for recently formed soils (Fedo et al., 1995).

Similarly, the base depletion index varied significantly among forest nutrient richness levels ($p < 0.01$) and increased significantly with depth ($p < 0.01$; Fig. 5). Base depletion index values, which are unitless ratios of base cation bearing to transition metal oxides, indicate the relative abundance of base-bearing minerals compared to the recalcitrant minerals. Rich sites exhibited the highest base depletion index (1.11), followed by poor sites (0.887), and moderate sites had the lowest (0.535). These values align with those reported in a study of volcanic soils, where base depletion indexes ranged from 0.83 to 1.53 (Anda et al., 2023). The higher base depletion index at rich sites reflects a greater abundance of base cations, likely due to the presence of Ca-plagioclase, apatite, and K feldspar minerals. Conversely, the lower base depletion index at nutrient poor sites can be attributed to the predominance of recalcitrant aluminosilicate minerals. The increase in base depletion index with depth suggests that base cations have been preferentially depleted from the upper soil horizons, possibly due to biological uptake and weathering processes.

3.2.5. *Enrichment-depletion of elements throughout the soil profile*

Understanding nutrient resupply to soil is important for ensuring sustainable forest harvesting and management practices. To investigate the influence of parent material mineralogy on nutrient depletion, mass transfer (τ) plots were created. These plots evaluate the enrichment or depletion of elements relative to their concentrations in uniform parent material, leveraging Ti as the reference element (Fig. 6; Supplemental Table 5). As previously noted, the uniformity of the parent material was determined using Zr/Ti ratios. Calcium τ values were all negative, indicating depletion compared to parent material, with the most depletion observed at the nutrient rich sites ($p < 0.01$). Soil Mg τ values were depleted in moderate sites but enriched in rich and poor sites compared to the parent material ($p < 0.01$). Soil K τ values were all positive, indicating enrichment relative to the parent material with a significant difference among forest nutrient richness ($p < 0.01$).

We expected to observe either a greater depletion of Ca, Mg, and K in the nutrient rich site due to the presence of more soluble minerals (e.g. Ca-plagioclase) or for the nutrient poor site to show greater depletion due to the low abundance and potential loss of minor nutrient-bearing minerals (e.g. apatite). Remarkably, the observed enrichment or depletion patterns for these elements were consistent across all forest nutrient richness levels throughout the soil profile (Fig. 4). We propose that the lack of significant Ca, Mg, and K depletion in nutrient rich sites can be attributed to the buffering effect of Ca-plagioclase weathering, as evidenced by the absence of strongly developed soil horizons like E and Spodic horizons, significantly higher pH, and significantly higher exchangeable Ca compared to the other richness levels. The base depletion index further supports this hypothesis, indicating a high abundance of base cations associated with cation-bearing minerals.

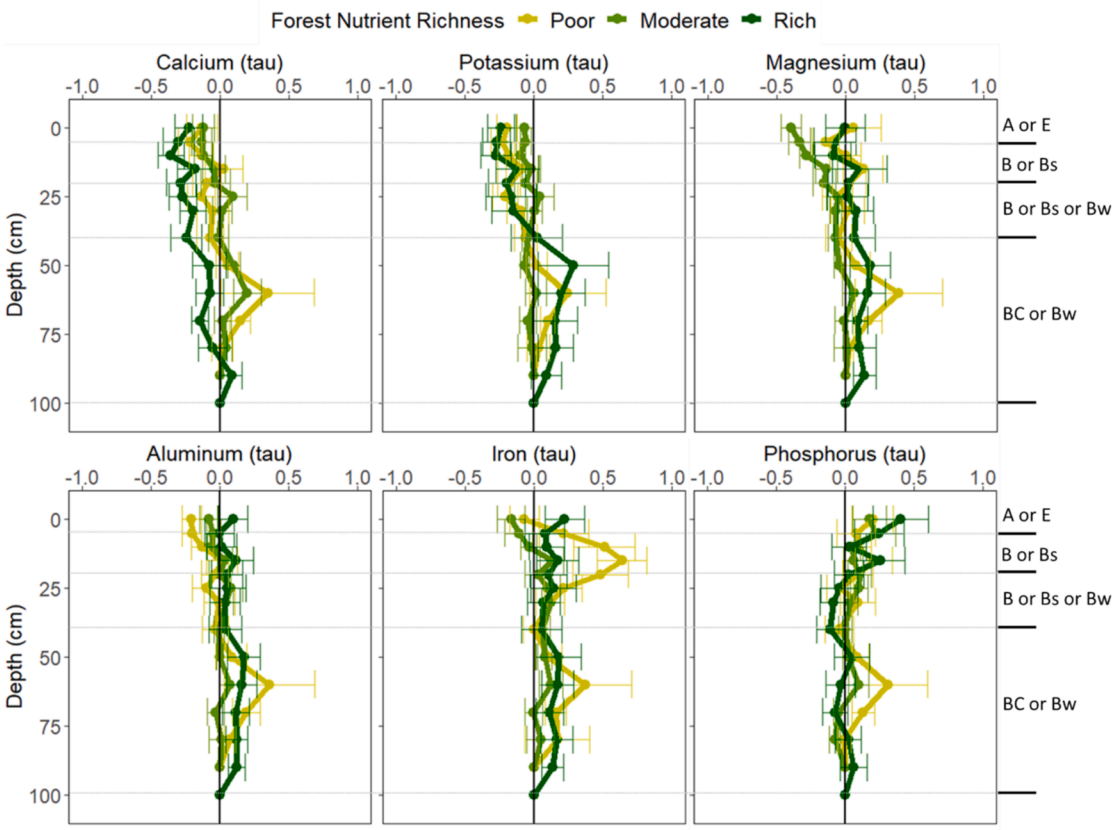

Fig. 6. Tau plots of total nutrients (via hydrofluoric digestion) standardized by the total nutrients of the parent material throughout the soil profile and across a nutrient richness gradient. The estimated soil horizons for the sites are delineated by a dashed gray line on the right. Each point represents the mean with error bars indicating the standard error.

Additionally, we hypothesize that the nutrient poor sites did not experience greater base cation depletion due to their predominance of recalcitrant aluminosilicate minerals. The lower chemical index of alteration in these soils suggests a less severe degree of weathering, but biological cycling may also be replenishing lost nutrient from the deeper horizons or through more efficient internal cycling.

Soil P τ values were also enriched across the nutrient richness gradient, but there were no significant differences among nutrient richness levels ($p = 0.80$). The enrichment of P in surface soils is very common in forested ecosystems due to biological uplift by trees, where this limited nutrient is tightly cycled compared to other nutrients. Within the northeastern United States, similar P enrichment was observed in Pennsylvania ranging from −0.25 to 1 in the A horizon (Kraepiel et al., 2015). Much of the A horizon was enriched in P which was contributed to from biological uplift or atmospheric inputs.

Overall, τ plot profiles for soil nutrients, except for P, did not follow soil organic matter or clay mineral content (Fig. 1; Fig. 6). Tau values for P were highest in the upper 20 cm of the mineral soil, which corresponds with higher soil organic matter. The enrichment of P and high organic matter suggests biological inputs, such as litterfall, are influencing the P in the upper mineral soil horizons. This is not surprising as the more organic matter in soil, the higher the sorption capacity for nutrients (Kang et al., 2009). This process involves active uptake by roots and recycling to the surface via litterfall, which contributes to an elevated nutrient abundance in the upper mineral soil horizons (Dijkstra and Smits, 2002; Xia et al., 2023). The significant interaction between nutrient richness and depth indicated that the effect of nutrient richness on nutrient concentrations varied depending on depth, with the exception of Al.

Total soil Al concentrations throughout the profile were enriched compared to parent material with the rich sites having the highest enrichment ($p < 0.01$). Overall, there were no extreme depletions or enrichments in total soil nutrients. Iron was mostly depleted compared to the parent material; however, nutrient moderate sites were the most depleted ($p < 0.01$). In the Bs horizon, Fe τ values were positive, indicating enrichment in comparison to the parent material. The enrichment is due to the accumulation of Fe oxides that are illuviated from the above A/E horizon at the poor and moderate sites.

3.3. Field soil weathering rates and batch reactor

3.3.1. Field soil solution

Dissolved organic carbon (DOC) and solution pH are critical factors influencing mineral weathering and adsorption processes in soil. To investigate the impact of parent material on elemental availability, we analyzed in-field soil solution chemistry. We found that DOC concentrations were significantly higher at the poor (8.66 mg/L) and moderate sites (7.35 mg/L) compared to the rich sites (3.57 mg/L; $p < 0.01$). These values fall within the range of similar studies reporting DOC concentrations (1.0 to 16.8 mg/L; Kerr and Eimers, 2012; Wilson et al., 2022). Conversely, soil solution pH was significantly higher at the rich sites (6.53) compared to the moderate (5.45) and poor sites (5.38; $p < 0.01$). These pH values fall within reported values that range from 3.5 to 6.9 (Armfield et al., 2019; Gruba and Mulder, 2008). We observed a negative correlation between DOC and soil solutions pH, suggesting that higher DOC concentrations may contribute to lower pH values in the soil solutions. This relationship is likely due to the formation of organic acids from the decomposition of organic matter, which can increase the acidity of the soil solution.

Elemental concentrations in soil solution are an important source of mineral nutrition for trees because they are easily drawn up via mass flow by tree roots. Overall, elemental concentrations were significantly influenced by forest nutrient richness ($p < 0.01$), except for K ($p = 0.37$), and P ($p = 0.71$; Fig. 7). Soil solution Ca concentrations were significantly higher at the rich site (16.0 mg/L) than both moderate (1.42 mg/L) and poor (0.852 mg/L; $p = 0.03$). Other studies have found Ca concentration in soil water ranging from 1.2 to 1.72 mg/L in the region (Armfield et al., 2019; McHale et al., 2002; Minocha et al., 2000; Porter et al., 2022). Magnesium concentrations were significantly higher at the rich (0.668 mg/L) and moderate (0.600 mg/L) sites than poor sites (0.217 mg/L; $p < 0.01$). Other studies have found Mg concentrations in soil water ranging from 0.2 to 0.51 mg/L in the region (McHale et al., 2002; Minocha et al., 2000; Porter et al., 2022). The rich sites are more than 10 times the upper extent of this range, most likely due to the high abundance of easily weathered Ca bearing minerals. These results are not surprising since the pH is buffered by Ca minerals in the soil. As pH decreases, Ca minerals are weathered and the hydrogen ions from organic acids are adsorbed, resulting in an increased or stable soil solution pH (Cincotta et al., 2019; Kerr and Eimers, 2012). Soil solution Ca and Mg concentrations were inversely correlated to DOC concentrations in the soil solution.

Soil solution K concentrations did not significantly differ across the forest nutrient richness gradient ($p = 0.36$). These results align with the soil exchangeable fraction and base cation saturation data, which were all higher for the nutrient rich site than the poor site. Other studies have found K concentration in soil water ranging from 0.1 to 2.35 mg/L in the region (McHale et al., 2002; Minocha et al., 2000; Porter et al., 2022). All nutrient concentrations were highest at the rich sites, which correlated to higher pH and negatively correlated with clay content (Fig. 1; Fig. 4). The low clay content and clay and mica minerals present in these soils suggests a reduced capacity to hold onto nutrients, potentially leading to higher concentrations of nutrients in the soil solutions. This effect may be exacerbated by the higher pH, which can indicate soil buffering and the reduced tendency of nutrients to be retained by clay minerals.

Soil solution P concentrations remain relatively consistent across the forest nutrient gradient, with no significant differences observed ($p = 0.71$). Concentrations ranged from 0.177 to 0.190 mg/L which are comparable to previous findings in the same region (Minocha et al., 2000). The lack of variation in soil solution P concentrations is consistent with the insignificant differences in exchangeable and total P concentrations across the nutrient richness gradient. This suggests that the limited abundance of P-bearing minerals, such as apatite, throughout the nutrient richness gradient exerts minimal influence on P availability in the soil solution; however it is possible that the apatite content in these soils is too low to detect a significant effect. Furthermore, soil solution P concentrations did not strongly correlate with soil solution pH or DOC concentrations, indicating that these factors have minimal influence on P availability at these sites.

Considering Al and Fe as a proxy for the combined effect of primary mineral dissolution and solubility of ions, our results highlight greater weathering and soluble ion transport at the poor and moderate site than the rich site. Moderate sites had significantly higher soil solution Al concentrations (0.714 mg/L) than poor (0.405 mg/L) and rich sites (0.101 mg/L; $p < 0.01$). Solution Al concentrations were greatest at the moderate site, despite lower soil pH at the poor site. Moreover, soil solution Al was significantly different between poor and moderate sites despite not being significantly different for the exchangeable Al soil profile. Other studies have found Al concentration in soil water ranging from 0.40 to 0.61 mg/L to in the region (Minocha et al., 2000; Porter et al., 2022). Soil solution Fe concentrations were significantly higher at the moderate sites (71.3 mg/mL) compared to the rich (0.043 mg/L) and poor sites (0.158 mg/mL; $p < 0.01$). Another study found Fe concentration in the region much lower at 0.0089 mg/L (Porter et al., 2022). We hypothesize the higher pH at the rich site decreased soluble Fe while the lower abundance of Fe bearing aluminosilicate minerals at the poor site limited soluble Fe at the poor site.

3.3.2. Estimated field nutrient release rates

Quantifying the field elemental release rates is important for understanding the loss of soil nutrients depending on parent material and our experimental design allows for an approximation. We estimated

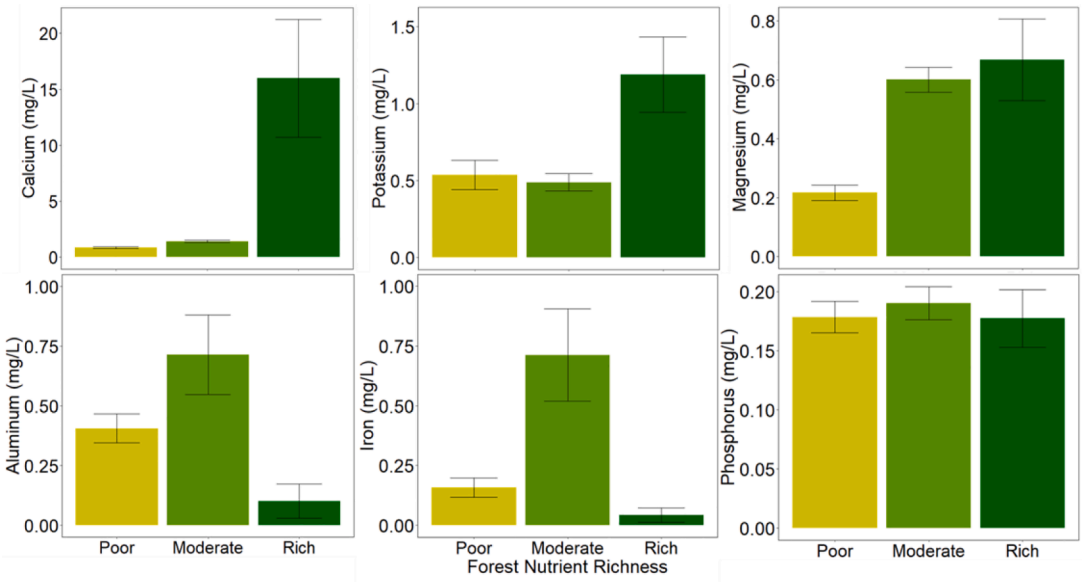

Fig. 7. Elemental concentrations in soil water collected from lysimeters. These averages with standard error bars are categorized by forest nutrient richness. Values used are from spring and fall 2022.

elemental release rates by scaling the soil water concentrations with soil volume, bulk density, surface area and yearly water fluxes. Our estimates (Fig. 8) suggest that elemental release rates did not differ among forest nutrient richness ($p > 0.05$) since there were no significant differences in nutrient release rates across the forest nutrient richness for Ca ($p = 0.27$), Mg ($p = 0.33$), K ($p = 0.74$), and P ($p = 0.28$). Although not significant, rates for Ca were higher for rich sites (6.12 mg/m^2/yr) than moderate (0.92 mg/cm^2/yr) and poor (0.89 mg/m^2/yr), which follows the same trend observed for soil water concentrations (Fig. 7). Release rates of Mg and K had comparable values across the nutrient richness gradient, which is a different result compared to soil water Mg and K concentrations (Fig. 7; Fig. 8). Estimated P release rates were inverse to the soil nutrient richness gradient and do not follow similar trends as the soil waters. These differences across the nutrient richness gradient were not significant because the variability was large within each forest nutrient richness, oftentimes greater than 50 % of the mean. The large variability was due to the upscaling of compounding errors from nutrient concentration, quantity of soil water collected, and bulk density heterogeneity among plots within a forest nutrient richness.

Field weathering rates for Al ($p = 0.13$) and Fe ($p = 0.28$) were also not statistically different across the forest nutrient richness gradient. Estimated Al release rates were highest at the poor site (0.38 mg/m^2/yr) with moderate sites in the middle (0.37 mg/cm^2/yr) and the rich sites having the lowest (0.0055 mg/m^2/yr). Estimated Fe release rates followed the same trajectory with rates the highest at the poor sites (0.52 mg/m^2/yr) and lowest at the rich sites (0.018 mg/m^2/yr). These rates were higher for poor and moderate sites than rich, which matches observations for soil water concentrations and is inverse to DOC concentrations. Overall, the estimated rates were highest where the soil pH was the lowest.

This is one of the first studies to estimate in-field release rates for inorganic nutrients by scaling annual soil water concentrations to soil

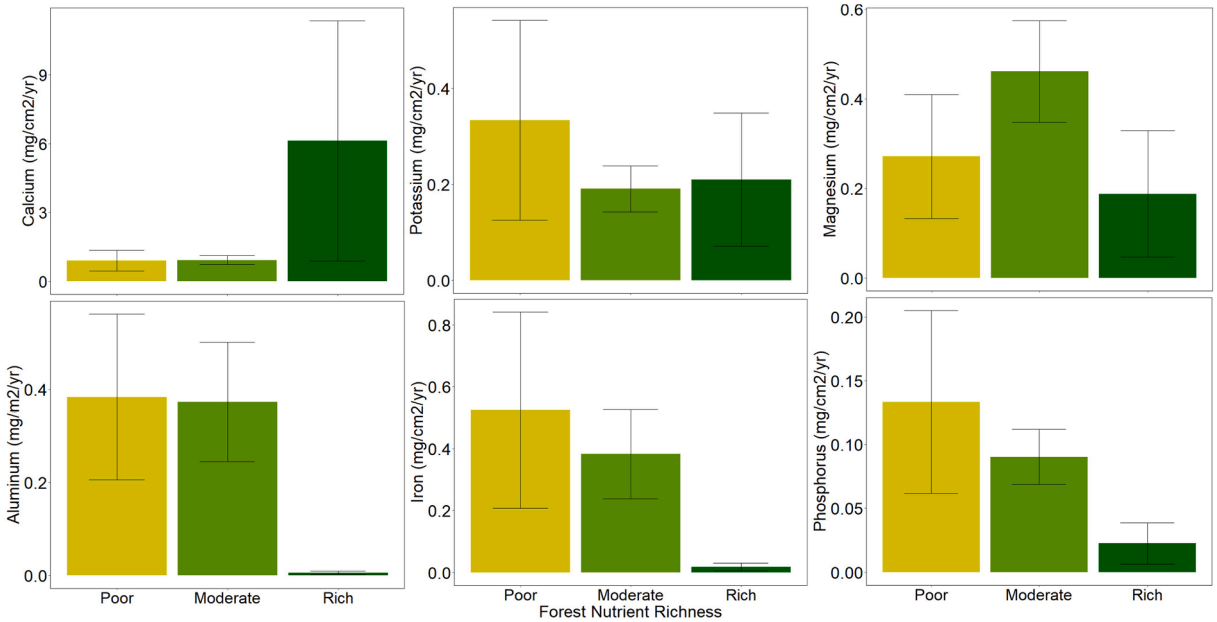

Fig. 8. In field soil weathering rates calculated from soil water solutions among forest nutrient richness. Error bars represent standard error.

volume. The majority of published "field" estimated weathering rates come from biogeochemical and Monte Carlo models (Futter et al., 2012), and laboratory experiments (Kolka et al., 1996) whereas ours uses field measurements to calculate the release rates. An assumption that our calculation makes is that all the released elements in the soil above the lysimeter are being collected, although that is not completely true because we do not account for tree uptake or lateral movement of soil water.

3.3.3. Batch reactor chemistry

While field-based weathering rate calculations can offer a valuable baseline for understanding weathering processes and nutrient availability in an ecosystem, laboratory experiments using batch reactors can provide a more controlled environment to assess nutrient release rates specifically from soil minerals without the complexities of forest floor dynamics and aboveground inputs. We found that nutrient release rates were significantly different across the forest nutrient richness gradient among soil materials and different depths ($p < 0.01$; Table 3; Supplemental Table 3). The Ca and Mg release rates were significantly different among the three forests with rich sites having higher rates than moderate, and poor sites ($p < 0.01$). Soil K release rates were significantly higher at rich sites (0.778 mg/m^2/day) than poor (0.550 mg/m^2/day), and moderate sites (0.462 mg/m^2/day; $p < 0.01$). The release rates of Ca, Mg, and K correspond to the exchangeable elemental concentrations of each in the soil, exhibiting the highest concentrations and release rates in the rich sites, a trend consistent with findings in a similar study (Street et al., 2023).

Contrary to the other elements, P release rates did not follow the nutrient gradient. Soil P release rates were highest at poor sites (10.1 mg/m^2/day) compared to rich (6.16 mg/m^2/day) and moderate sites (4.96 mg/m^2/day: $p < 0.01$). Since P bearing minerals were in low abundance in the parent material, our results suggest that P adsorption to soil surfaces is more pronounced at the poor sites than the rich and moderate, which is supported by another study in the region (Street et al., 2023). Additionally, the higher Ca concentrations in the moderate and rich sites may induce Ca-P bearing mineral precipitation since this reaction is primarily governed by the Ca concentration and pH in the soil (Tunesi et al., 1999).

Using Al and Fe as a proxy for aluminosilicate and ferrosilicate weathering, we expected higher release rates at the poor site due to lower base cation buffering and match our field observations. However, we found release rates of Al were significantly higher at rich (6.3 mg/m^2/day) and poor (5.9 mg/m^2/day) sites than moderate (4.3 mg/m^2/day; $p < 0.01$). Similarly, the Fe release rates were significantly higher in poor (13.4 mg/m^2/day) and rich (10.3 mg/m^2/day) sites compared to the moderate sites (7.2 mg/m^2/day; $p < 0.01$). Higher Al release rates at the rich site indicated higher aluminosilicate weathering rates, supporting the idea of Ca-plagioclase weathering buffering pH and supporting the idea that base cation saturation and pH promote nutrient adsorption. Higher Fe release rates at the poor site contributed to secondary Fe oxide dissolution due to the low pH.

Overall, we saw greater release rates at the surface rather than with depth (Table 3; Supplemental Table 3). Greater release rates at the surface may be attributed to the increased exposure and easier weathering of already weathered mineral surfaces, despite the deeper soils undergoing weathering of more soluble minerals typically hypothesized as important elemental sources.

Solution acidity had significant effects on elemental release rates from soil. There were no effects of pH on Ca ($p = 0.05$) or P ($p = 0.38$) release rates from soil. Soil Mg release rates were significantly affected by solution acidity, with pH 4 releasing an average of 2.19 mg/m^2/day, pH 5 at 1.27 mg/m^2/day, and pH 6 at 0.888 mg/m^2/day ($p < 0.01$). Similarly, K release rates were significantly higher at pH 4 (0.711 mg/m^2/day) than at pH 6 (0.510 mg/m^2/day), but not at pH 5 (0.568 mg/m^2/day; $p < 0.01$). Soil acidity and Ca concentrations in soils affect the precipitation of Ca-P bearing minerals, which might affect the measurable P in solution (Tunesi et al., 1999), or because of the small ionic radius P may be adsorbed to soil surfaces after being released into solution (Street et al., 2023). Soil Al release rates were also affected by solution acidity, with pH 4 (7.96 mg/m^2/day) significantly increasing rates compared to pH 5 (4.62 mg/m^2/day) and pH 6 (4.02 mg/m^2/day; $p < 0.01$). Soil Fe release rates were highest with pH 4 (14.5 mg/m^2/

Table 3
Batch reactor average release rates of inorganic nutrients from soils with varying pH among three depth ranges. These averages were calculated from the last 28-days of the 70-day total experiment because once steady state had been achieved. Each treatment average consists of six replicates with reported standard error (±).

Soil Nutrient Richness	Depth Range (cm)	Initial pH	*Soil Nutrients Release Rate (mg/m^2/d)*					
			Al	Fe	Ca	K	Mg	P
Rich	5–10	4	10.9 (±2.3)	36.6 (±9.4)	0.196 (±0.030)	0.894 (±0.074)	0.785 (±0.19)	11.05 (±4.8)
		5	4.95 (±0.66)	19.3 (±4.9)	0.180 (±0.026)	0.658 (±0.13)	0.286 (±0.055)	10.53 (±4.7)
		6	3.99 (±0.61)	17.4 (±4.7)	0.152 (±0.026)	0.566 (±0.081)	0.192 (±0.033)	10.2 (±4.5)
	30–40	4	9.15 (±1.2)	13.6 (±0.92)	0.158 (±0.014)	0.565 (±0.072)	0.560 (±0.067)	11.0 (±4.8)
		5	5.62 (±1.1)	8.65 (±1.3)	0.155 (±0.023)	0.500 (±0.050)	0.236 (±0.023)	11.4 (±5.1)
		6	6.46 (±1.5)	7.26 (±1.1)	0.164 (±0.041)	0.587 (±0.081)	0.184 (±0.023)	10.7 (±4.8)
	80–90	4	5.78 (±0.85)	8.70 (±0.85)	0.163 (±0.037)	0.433 (±0.042)	0.700 (±0.095)	8.58 (±3.8)
		5	3.28 (±0.55)	4.91 (±0.92)	0.213 (±0.079)	0.356 (±0.048)	0.280 (±0.063)	9.26 (±4.1)
		6	3.55 (±0.6)	3.79 (±0.65)	0.242 (±0.10)	0.388 (±0.053)	0.177 (±0.038)	8.33 (±3.8)
Moderate	5–10	4	8.55 (±1.2)	13.8 (±2.1)	0.985 (±0.11)	0.381 (±0.076)	2.43 (±0.42)	6.56 (±2.8)
		5	6.42 (±0.96)	11.5 (±2.2)	0.824 (±0.068)	0.316 (±0.070)	1.72 (±0.33)	6.63 (±2.8)
		6	6.16 (±0.85)	10.8 (±1.7)	0.918 (±0.19)	0.238 (±0.033)	1.22 (±0.26)	5.97 (±2.5)
	30–40	4	6.05 (±0.75)	9.39 (±1.2)	1.365 (±0.19)	0.660 (±0.12)	2.967 (±0.27)	6.64 (±2.8)
		5	3.51 (±0.43)	6.51 (±0.65)	1.122 (±0.14)	0.551 (±0.075)	1.88 (±0.19)	5.99 (±2.6)
		6	3.53 (±0.64)	6.88 (±1.1)	0.870 (±0.076)	0.54 (±0.081)	1.60 (±0.18)	6.11 (±2.6)
	80–90	4	10.9 (±1.51)	15.2 (±2.0)	1.721 (±0.26)	1.75 (±0.66)	6.28 (±1.29)	5.76 (±2.4)
		5	6.74 (±1.6)	10.4 (±2.1)	1.18 (±0.14)	1.43 (±0.63)	4.41 (±1.26)	6.12 (±2.6)
		6	4.95 (±1.0)	8.04 (±1.4)	0.751 (±0.030)	1.14 (±0.46)	3.19 (±0.80)	5.63 (±2.4)
Poor	5–10	4	5.16 (±1.3)	9.82 (±2.7)	0.315 (±0.047)	0.404 (±0.084)	1.26 (±0.31)	5.21 (±2.3)
		5	2.77 (±0.41)	5.54 (±1.0)	0.361 (±0.036)	0.319 (±0.062)	0.54 (±0.094)	5.74 (±2.5)
		6	2.20 (±0.35)	4.65 (±1.2)	0.246 (±0.023)	0.323 (±0.050)	0.332 (±0.049)	6.12 (±2.7)
	30–40	4	9.53 (±1.2)	14.3 (±1.1)	0.318 (±0.11)	0.701 (±0.15)	2.81 (±0.23)	5.87 (±2.6)
		5	5.49 (±1.1)	8.43 (±0.81)	0.473 (±0.13)	0.561 (±0.13)	1.25 (±0.10)	5.98 (±2.6)
		6	3.57 (±0.67)	5.66 (±0.71)	0.455 (±0.088)	0.458 (±0.088)	0.653 (±0.068)	5.82 (±2.5)
	70–80	4	5.58 (±0.70)	8.74 (±0.98)	0.735 (±0.11)	0.613 (±0.15)	1.95 (±0.15)	3.43 (±1.4)
		5	2.80 (±0.30)	4.78 (±0.37)	0.694 (±0.044)	0.424 (±0.079)	0.853 (±0.038)	3.401 (±1.4)
		6	1.81 (±0.20)	2.67 (±0.23)	0.494 (±0.022)	0.358 (±0.060)	0.433 (±0.040)	3.09 (±1.3)

day) compared to pH 5 (8.89 mg/m^2/day) and pH 6 (7.46 mg/m^2/day; $p < 0.01$).

From our batch reactor experiments, we found a correspondence of parent material and solution chemistry to nutrient release rates from soil. Parent materials with high total Ca, and Mg concentrations exhibited higher release rates, typically corresponding to rich sites. Additionally, soil acidity influenced release rates, with more acidic solutions releasing more elements from minerals in the soil. Understanding the controls and influences of weathering rates is crucial for accurate nutrient budget calculation. Therefore, our finding that nutrient release rates were controlled by both soil solution acidity and parent material mineralogy is important and is supported by other studies that found effects of both pH and mineralogy on elemental release rates (Casetou-Gustafson et al., 2019; Richardson and Zuñiga, 2021; Zhang et al., 2019). Additionally, the batch reactor release rates were one to five orders of magnitude larger than the estimate in field rates, most likely due to ecosystem dynamics such as plant uptake and lateral flow that are not present in the laboratory. Unfortunately, our batch reactor experiment highlighted that the in-field weathering estimates were only useful when soil nutrients were high, in the case of Ca from Ca-plagioclase or very low, in the case of P from apatite; although this does provide a useful, cost-effective tool for estimating relative release rates across sites.

4. Synthesis and conclusions

Our study explored the influence of parent material on soil nutrient concentrations and their release rates in northern hardwood forests of New England, USA. We found a strong link between the abundance of Ca and Mg- bearing minerals in the parent material and their total and exchangeable fraction in the soil and led to higher soil pH and base cation saturation. All of these factors promote the growth of northern hardwood trees. Our EPMA data revealed that the Ca and Mg gradient is generated from an abundance of Ca-plagioclase, mica, and amphibole minerals, rather than carbonates as typically hypothesized. Despite the differences in Ca and Mg bearing minerals and total and exchangeable concentrations, we did not detect significant differences in soil water Ca and Mg concentrations along the nutrient gradient. The Ca and Mg rich sites were about six times greater than those at the poor and moderate sites but were not significantly different due to spatial heterogeneity. The high Ca concentration in soil water might indicate enhanced acid buffering capacity, even though carbonates were not detected by EPMA. This suggests greater Ca availability to trees at the rich sites in solution and in solid phase, which likely contributes to higher overall site productivity, especially through tree growth.

Soil total K and P followed a different pattern than Ca and Mg. Total K concentrations were highest at the Ca-Mg poor site, indicating the importance of K feldspar in controlling soil K concentrations. However, exchangeable K concentrations positively corresponded with increased site nutrient richness. This likely reflects the combined effects of increasing CEC and soil pH, which promote the availability of K for plant uptake. Even though nutrient rich sites have lower abundance of K-bearing minerals, the increased availability due to higher CEC and pH make them less likely to be K limited for tree growth. Total P was lowest at the poor sites across sites but had comparable abundances of apatite therefore other P bearing aluminosilicate minerals are the major source of P in these soils. Exchangeable P concentrations were highest at the moderate site, likely due to the combined effects of clay content and Fe concentrations, which are known to influence P adsorption. Despite these differences in exchangeable P, no significant differences were observed in soil water P concentrations. This finding suggests that P sorption with Fe and Al is occurring at the nutrient rich site, evident from the pH, and low Fe and Al concentrations in the soil water. These results highlight the importance of considering soil properties like pH, CEC, Fe, and Al concentrations since these factors influence K and P availability, which impacts the accessibility by plants.

Assessing the impact of weathering on nutrient release was an important goal of this work. We expected that greater acidity and lower Ca and Mg abundance may lead to overall faster depletion rates at the nutrient poor site compared to the rich site. Interestingly, soil profile τ values revealed similar levels of depletion and enrichment for all elements (Ca, Mg, K, and P) across the nutrient richness gradient, suggesting that both the soil buffering capacity and the resistance of minerals to weathering influence release rates. We compared field weathering rates obtained from lysimeter water with laboratory batch reactor experiments. While the calculated field nutrient release rates were one to two orders of magnitude lower (Ca, Mg, K) or five orders of magnitude lower (P) than in the laboratory experiment, the relative trend in nutrient richness among sites was consistent across both methods. The estimated field nutrient release rates were much lower than the laboratory experiment because of ecosystem dynamics such as plant uptake and lateral flow that remove elements from solution before leaching through the soil profile. The laboratory-based batch reactor study indicated that Ca and Mg nutrient release rates corresponded to their soil total concentration but, P was significantly higher at the poor sites, suggesting a greater influence of mineral phases. These trends were amplified by increased soil water acidity. While total elemental concentrations provide a basic understanding, soil characteristics like mineralogy and pH play a crucial role in mineral weathering, sorption and ultimately the accessibility of nutrients for tree growth.

Our study highlights the critical role of parent material mineralogy, particularly minerals rich in Ca and Mg, in controlling nutrient release rates and influencing long-term forest productivity. These minerals promote higher base saturation in the soil, making essential nutrients like Ca and Mg readily available for tree uptake, thus enhancing site productivity. Interestingly, we initially anticipated carbonate minerals to be the primary Ca source in these forests, however, no carbonate minerals were detected through EPMA. Therefore, their role in release rates appears less significant than expected. Consequently, sites with parent material rich in Ca-plagioclase, mica, and amphibole minerals may be suitable for supporting shorter timber harvesting rotations while maintaining soil health and nutrient supply over extended time frames. However, further research on aboveground productivity is warranted to fully understand these implications for sustainable forest management practices.

CRediT authorship contribution statement

Alexandrea M. Rice: Writing – review & editing, Writing – original draft, Visualization, Validation, Software, Resources, Methodology, Formal analysis, Data curation. **Nicolas Perdrial:** Writing – review & editing, Writing – original draft, Visualization, Validation, Software, Resources, Methodology, Investigation, Funding acquisition, Formal analysis, Data curation, Conceptualization. **Victoria Treto:** Writing – review & editing, Software, Methodology, Data curation. **Anthony W. D'Amato:** Writing – review & editing, Resources, Project administration, Methodology, Investigation, Funding acquisition, Data curation, Conceptualization. **Grace A. Smith:** Writing – review & editing, Resources, Methodology, Data curation. **Justin B. Richardson:** Writing – review & editing, Writing – original draft, Supervision, Resources, Project administration, Methodology, Investigation, Funding acquisition, Formal analysis, Data curation, Conceptualization.

Declaration of competing interest

The authors declare that they have no known competing financial interests or personal relationships that could have appeared to influence the work reported in this paper.

Acknowledgements

We thank the 2021 soil pit crew for all their efforts helping dig soil

pits and sampling soils. Thank you to Marissa Hanley, Rhea Negron, Wenxiu Teng, Bailee Street, Trevor Mackowiak, Bren Cable, Eve Foran, and Christopher Marshall, for their assistance collecting and processing soil waters. A special thank you to John Sweeney for building essential equipment and items for this project, Kevin Evans for assistance in locating field sites, and William Leak, Mariko Yamasaki, and Chris Costello for creating and stewarding severl of the long-term experiments used for this work. This study was funded by the USDA National Institute of Food and Agriculture Grant 2021-67019-34250 with long-term silviculture studies at the Bartlett Experimental Forest supporting this project funded by the USDA Forest Service Northern Research Station.

Appendix A. Supplementary data

Supplementary data to this article can be found online at https://doi.org/10.1016/j.geoderma.2024.117081.

Data availability

Data will be made available on request.

References

Achat, D.L., Deleuze, C., Landmann, G., Pousse, N., Ranger, J., Augusto, L., 2015. Quantifying consequences of removing harvesting residues on forest soils and tree growth - a meta-analysis. For. Ecol. Manage. 348, 124–141. https://doi.org/10.1016/j.foreco.2015.03.042.

Achat, D.L., Martel, S., Picart, D., Moisy, C., Augusto, L., Bakker, M.R., Loustau, D., 2018. Modelling the nutrient cost of biomass harvesting under different silvicultural and climate scenarios in production forests. For. Ecol. Manage. 429, 642–653. https://doi.org/10.1016/j.foreco.2018.06.047.

Adams, M.B., Kelly, C., Kabrick, J., Schuler, J., 2019. Temperate forests and soils (pp. 83–108). https://doi.org/10.1016/b978-0-444-63998-1.00006-9.

Álvarez, E., Fernández-Marcos, M.L., Monterroso, C., Fernández-Sanjurjo, M.J., 2005. Application of aluminium toxicity indices to soils under various forest species. In: Forest Ecology and Management (Vol. 211, Issue 3, pp. 227–239). https://doi.org/10.1016/j.foreco.2005.02.044.

Anda, M., Purwanto, S., Dariah, A., Watanabe, T., Dahlgren, R.A., 2023. A 200-year snapshot of soil development in pyroclastic deposits derived from the 1815 super explosive eruption of Mount Tambora in Indonesia. Geoderma 433. https://doi.org/10.1016/j.geoderma.2023.116454.

April, R., Newton, R., 1992. Mineralogy and Mineral Weathering. In: Atmospheric Deposition and Forest Nutrient Cycling. Springer, pp. 378–425.

Armfield, J.R., Perdrial, J.N., Gagnon, A., Ehrenkranz, J., Perdrial, N., Cincotta, M., Ross, D., Shanley, J.B., Underwood, K.L., Ryan, P., 2019. Does stream water composition at sleepers river in vermont reflect dynamic changes in soils during recovery from acidification? Front. Earth Sci. 6. https://doi.org/10.3389/feart.2018.00246.

Asmare, T.K., Abayneh, B., Yigzaw, M., Birhan, T.A., 2023. The effect of land use type on selected soil physicochemical properties in Shihatig watershed, Dabat district. Northwest Ethiopia. Heliyon 9 (5). https://doi.org/10.1016/j.heliyon.2023.e16038.

Augusto, L., Achat, D.L., Bakker, M.R., Bernier, F., Bert, D., Danjon, F., Khlifa, R., Meredieu, C., Trichet, P., 2015. Biomass and nutrients in tree root systems-sustainable harvesting of an intensively managed Pinus pinaster (Ait.) planted forest. GCB Bioenergy 7 (2), 231–243. https://doi.org/10.1111/gcbb.12127.

Barnes, W.A., Quideau, S.A., Swallow, M.J.B., 2018. Nutrient distribution in sandy soils along a forest productivity gradient in the athabasca oil sands region of Alberta, Canada. Canad. J. Soil Sci. 98 (2), 277–291. https://doi.org/10.1139/cjss-2017-0074.

Bennett, D.S., Wittkop, C.A., Dicken, C.L., 2006. Bedrock Geologic Map of New Hampshire - A Digital Representation of the Lyons and others 1997 map and ancillary files: U.S. Geological Survey Data Series 215 scale 1:250,000.

Boerner, R.E.J., Morris, S.J., Decker, K.L.M., Hutchinson, T.F., 2003. Soil and Forest Floor Characteristics.

Bojórquez-Quintal, E., Escalante-Magaña, C., Echevarría-Machado, I., Martínez-Estévez, M., 2017. Aluminum, a friend or foe of higher plants in acid soils. In: Frontiers in Plant Science (Vol. 8). Frontiers Media S.A. https://doi.org/10.3389/fpls.2017.01767.

Bonar, A.L., Soreghan, G.S., Elwood Madden, M.E., 2023. Assessing weathering, pedogenesis, and silt generation in granitoid-hosted soils from contrasting hydroclimates. J. Geophys. Res. Earth 128 (7). https://doi.org/10.1029/2023JF007095.

Bowden, R.D., Wurzbacher, S.J., Washko, S.E., Wind, L., Rice, A.M., Coble, A.E., Baldauf, N., Johnson, B., Wang, J., Simpson, M., Lajtha, K., 2019. Long-term Nitrogen Addition Decreases Organic Matter Decomposition and Increases Forest Soil Carbon. Soil Sci. Soc. Am. J. 83 (S1). https://doi.org/10.2136/sssaj2018.08.0293.

Bower, J.A., Ross, D.S., Bailey, S.W., Pennino, A.M., Jercinovic, M.J., McGuire, K.J., Strahm, B.D., Schreiber, M.E., 2023. Development of a lateral topographic weathering gradient in temperate forested podzols. Geoderma 439. https://doi.org/10.1016/j.geoderma.2023.116677.

Brantley, S.L., Lebedeva, M., 2011. Learning to read the chemistry of regolith to understand the critical zone. Annu. Rev. Earth Planet. Sci. 39, 387–416. https://doi.org/10.1146/annurev-earth-040809-152321.

Brimhall, G.H., Dietrich, W.E., 1986. Constitutive mass balance relations between chemical composition, volume, density, porosity, and strain in metasomatic hydrochemkai systems: Results on weathering and pedogenesis. Geochim. Cosmochim. Acta 51, 567–587.

Casetou-Gustafson, S., Akselsson, C., Hillier, S., Olsson, B.A., 2019. The importance of mineral determinations to PROFILE base cation weathering release rates: a case study. Biogeosciences 16 (9), 1903–1920. https://doi.org/10.5194/bg-16-1903-2019.

Cincotta, M.M., Perdrial, J.N., Shavitz, A., Libenson, A., Landsman-Gerjoi, M., Perdrial, N., Armfield, J., Adler, T., Shanley, J.B., 2019. Soil aggregates as a source of dissolved organic carbon to streams: an experimental study on the effect of solution chemistry on water extractable carbon. Front. Environ. Sci. 7. https://doi.org/10.3389/fenvs.2019.00172.

Cleavitt, N.L., Battles, J.J., Johnson, C.E., Fahey, T.J., 2018. Long-term decline of sugar maple following forest harvest, Hubbard Brook Experimental Forest, New Hampshire. Can. J. For. Res. 48 (1), 23–31. https://doi.org/10.1139/cjfr-2017-0233.

Coile, T.S., 1952. Soil and the Growth of Forests. Adv. Agron. 4, 329–398.

Cronan, C.S., Grigal, D.F., 1995. Use of calcium/aluminum ratios as indicators of stress in forest ecosystems. J. Environ. Qual. 24 (2), 209–226. https://doi.org/10.2134/jeq1995.00472425002400020002x.

Dijkstra, F.A., Smits, M.M., 2002. Tree species effects on calcium cycling: The role of calcium uptake in deep soils. Ecosystems 5 (4), 385–398. https://doi.org/10.1007/s10021-001-0082-4.

Dijkstra, F.A., Van Breemen, N., Jongmans, A.G., Davies, G.R., Likens, G.E., 2003. Calcium weathering in forested soils and the effect of different tree species. Biogeochemistry 62, 253–275.

Dragun, J., 1988. The Soil Chemistry of Hazardous Materials. Hazardous Materials Control Research Institute. Silver, Spring, MD USA.

Eberl, D.D., Smith, D.B., 2009. Mineralogy of soils from two continental-scale transects across the United States and Canada and its relation to soil geochemistry and climate. Appl. Geochem. 24 (8), 1394–1404. https://doi.org/10.1016/j.apgeochem.2009.04.010.

Ericsson, T., 1994. Nutrient dynamics and requirements of forest crops. N. Z. J. For. Sci. 24 (2/3), 133–168.

Federer, C.A., Hornbeck, J.W., 1985. The buffer capacity of forest soils in New England. Water Air Soil Pollut. 26, 163–173.

Fedo, C.M., Wayne Nesbitt, H., Young, G.M., 1995. Unraveling the effects of potassium metasomatism in sedimentary rocks and paleosols, with implications for paleoweathering conditions and provenance. Geology 23 (10), 921–924. https://doi.org/10.1130/0091-7613(1995)023<0921:uteopm>2.3.co;2.

Fink, J. R., Inda, A. V., Tiecher, T., & Barrón, V. (2016). Iron oxides and organic matter on soil phosphorus availability. In Ciencia e Agrotecnologia (Vol. 40, Issue 4, pp. 369–379). Federal University of Lavras. https://doi.org/10.1590/1413-70542016404023016.

Finzi, A.C., Canham, C.D., van Breemen, N., 1998. Canopy tree-soil interactions within temperate forests: species effects on ph and cations. Ecol. Appl. 8 (2), 447. https://doi.org/10.2307/2641084.

Futter, M.N., Klaminder, J., Lucas, R.W., Laudon, H., Köhler, S.J., 2012. Uncertainty in silicate mineral weathering rate estimates: Source partitioning and policy implications. Environ. Res. Lett. 7 (2). https://doi.org/10.1088/1748-9326/7/2/024025.

Garrett, L.G., Smaill, S.J., Beets, P.N., Kimberley, M.O., Clinton, P.W., 2021. Impacts of forest harvest removal and fertiliser additions on end of rotation biomass, carbon and nutrient stocks of Pinus radiata. For. Ecol. Manage. 493. https://doi.org/10.1016/j.foreco.2021.119161.

Gee, G.W. & Bauder, J.W. (1986) Particle-Size Analysis. In: Klute, A., Ed., Methods of Soil Analysis, Part 1. Physical and Mineralogical Methods, Agronomy Monograph No. 9, 2nd Edition, American Society of Agronomy/Soil Science Society of America, Madison, WI, 383-411.

Goldich, S.S., 1938. A study in rock-weathering. J. Geol. 46, 17–58.

Goyne, K.W., Brantley, S.L., Chorover, J., 2006. Effects of organic acids and dissolved oxygen on apatite and chalcopyrite dissolution: Implications for using elements as organomarkers and oxymarkers. Chem. Geol. 234 (1–2), 28–45. https://doi.org/10.1016/j.chemgeo.2006.04.003.

Gradowski, T., Thomas, S.C., 2006. Phosphorus limitation of sugar maple growth in central Ontario. For. Ecol. Manage. 226 (1–3), 104–109. https://doi.org/10.1016/j.foreco.2005.12.062.

Gruba, P., Mulder, J., 2008. Relationship between Aluminum in Soils and Soil Water in Mineral Horizons of a Range of Acid Forest Soils. Soil Sci. Soc. Am. J. 72 (4), 1150–1157. https://doi.org/10.2136/sssaj2007.0041.

Hazlett, P., Emilson, C., Lawrence, G., Fernandez, I., Ouimet, R., Bailey, S., 2020. Reversal of forest soil acidification in the Northeastern United States and Eastern Canada: Site and soil factors contributing to recovery. Soil Systems 4 (3), 1–22. https://doi.org/10.3390/soilsystems4030054.

Heřmanská, M., Voigt, M.J., Marieni, C., Declercq, J., Oelkers, E.H., 2022. A comprehensive and internally consistent mineral dissolution rate database: Part I: Primary silicate minerals and glasses. Chem. Geol. 597.

Hornbeck, D.A., Sullivan, D.M., Owen, J., & Hart, J.M. (2019). Soil Test Interpretation Guide. EC 1478. Corvallis, OR: Oregon State University Extension Service.

Hornbeck, J.W., Smith, C.T., Martin, C.W., Tritton, L.M., Pierce, R.S., 1990. Effects of Intensive Harvesting on Nutrient Capitals of Three Forest Types in New England. 30, 55–64.
Hornbeck, D.A., Sullivan, D.M., Owen, J., Hart, J.M., 2019. Soil Test Interpretation Guide. EC 1478. Oregon State University Extension Service, Corvallis, OR.
Jackson, K., Thomas Meetei, T., 2018. Influence of soil pH on nutrient availability: a review. J. Emerg. Technol. Innov. Res. 5 (12), 707–713 www.jetir.org.
Jenny, H., 1941. Factors of Soil Formation: A System of Quantitative Pedology. Dover Publications, New York, p. 281.
Jien, S.H., Baillie, I., Huang, W.S., Chen, Y.Y., Chiu, C.Y., 2016. Incipient ferralization and weathering indices along a soil chronosequence in Taiwan. Eur. J. Soil Sci. 67 (5), 583–596. https://doi.org/10.1111/ejss.12363.
JMP®, Version 17. SAS Institute Inc., Cary, NC, 1989–2023.
Jordan, C.F., 1968. A simple, tension free lysimeter. Soil Sci. 105 (2), 81–86. https://doi.org/10.1097/00010694-196802000-00003.
Kaiser, W.M., 1982. Correlation between changes in photosynthetic activity and changes in total protoplast volume in leaf tissue from hygro-, meso- and xerophytes under osmotic stress. Planta 154, 538–545. https://doi.org/10.1007/BF00402997.
Kang, J., Hesterberg, D., Osmond, D.L., 2009. Soil organic matter effects on phosphorus sorption: a path analysis. Soil Sci. Soc. Am. J. 73 (2), 360–366. https://doi.org/10.2136/sssaj2008.0113.
Kaupenjohann, M., Zech, W., Hantschel, R., Horn, R., Schneider, B.U., 1989. Mineral Nutrition of Forest Trees: A Regional Survey. In: Schulze, E.-.-D., Lange, O.L., Oren, R. (Eds.), Forest Decline and Air Pollution, Vol. 77. Springer, Berlin Heidelberg, pp. 282–294. https://doi.org/10.1007/978-3-642-61332-6.
Kelly, E.F., Chadwick, O.A., Hilinski, T.E., 1998. The effect of plants on mineral weathering. Biogeochemistry 42, 21–53.
Kerr, J.G., Eimers, M.C., 2012. Decreasing soil water Ca 2+ reduces DOC adsorption in mineral soils: Implications for long-term DOC trends in an upland forested catchment in southern Ontario, Canada. Sci. Total Environ. 427–428, 298–307. https://doi.org/10.1016/j.scitotenv.2012.04.016.
Kolka, R.K., Grigal, D.F., Nater, E.A., 1996. Forest soil mineral weathering rates: use of multiple approaches. Geoderma 73. ELSEVIER.
Koteff, C., Pessl, F., 1981. Systematic Ice Retreat in New England. Geological Survey Professional Paper 1179.
Kraepiel, A.M.L., Dere, A.L., Herndon, E.M., Brantley, S.L., 2015. Natural and anthropogenic processes contributing to metal enrichment in surface soils of central Pennsylvania. Biogeochemistry 123 (1–2), 265–283. https://doi.org/10.1007/s10533-015-0068-5.
Li, H., Zhao, Y., Weng, X., Zhou, Y., Zhang, S., Liu, L., Pei, J., 2023. The Most Suitable Calcium Concentration for Growth Varies among Different Tree Species—Taking Pinus tabuliformis, Pinus sylvestris var. mongolica, Populus, and Morus alba as Examples. Forests 14 (7). https://doi.org/10.3390/f14071437.
Liese, H.C., 1973. Mineral Composition of the Conway Granite in New Hampshire. GSA Bull. 84, 331–334.
Likens, G.E., Driscoll, C.T., Buso, D.C., Siccama, T.G., Johnson, C.E., Lovett, G.M., Fahey, T.J., Reiners, W.A., Ryan, D.F., Martin, C.W., Bailey, S.W., 1998. The biogeochemistry of calcium at Hubbard Brook. Biogeochemistry 41.
Liu, X., Meng, W., Liang, G., Li, K., Xu, W., Huang, L., Yan, J., 2014. Available phosphorus in forest soil increases with soil nitrogen but not total phosphorus: Evidence from subtropical forests and a pot experiment. PLoS One 9 (2). https://doi.org/10.1371/journal.pone.0088070.
Lyons, J.B., Bothner, W.A., Moench, R.H., Thompson Jr., J.B., 1997 Bedrock geologic map of New Hampshire. U.S. Geological Survey. https://doi.org/10.3133/70211051.
Manning, D.A.C., 2022. Mineral stabilities in soils: how minerals can feed the world and mitigate climate change. Clay Miner. 57 (1), 31–40. https://doi.org/10.1180/clm.2022.17.
Marsan, F.A., Bain, D.C., Duthie, D.M.L., 1988. Parent material uniformity and degree of weathering in a soil chronosequence, Northwestern Italy. Catena 15, 507–517. https://doi.org/10.1016/0341-8162(88)90002-1.
McHale, M.R., McDonnell, J.J., Mitchell, M.J., Cirmo, C.P., 2002. A field-based study of soil water and groundwater nitrate release in an Adirondack forested watershed, 2–1-2–16 Water Resour. Res. 38 (4). https://doi.org/10.1029/2000wr000102.
McKenzie, N.N., Jacquier, D.D., Isbell, R.R., Brown, K.K., 2004. Austrailian Soils and Landscapes. CSIRO Publishing, pp. 1–433.
Minocha, R., Long, S., Magill, A. H., Aber, J., & Mcdowell, W. H. (2000). Foliar free polyamine and inorganic ion content in relation to soil and soil solution chemistry in two fertilized forest stands at the Harvard Forest, Massachusetts. In Plant and Soil (Vol. 222).
Morris, D.M., Kwiaton, M.M., Duckert, D.R., 2014. Black spruce growth response to varying levels of biomass harvest intensity across a range of soil types: 15-year results. Can. J. For. Res. 44 (4), 313–325. https://doi.org/10.1139/cjfr-2013-0359.
Nesbitt, H.W., Young, G.M., 1982. Early Proterozoic climates and plate motions inferred from major element chemistry of Intites. Nature 299, 715–717.
Nesbitt, H.W., Young, G.M., 1989. Formation and Diagenesis of Weathering Profiles. J. Geol. 97 (2), 129–147. http://www.journals.uchicago.edu/t-and-c.
Nezat, C.A., Blum, J.D., Klaue, A., Johnson, C.E., Siccama, T.G., 2004. Influence of landscape position and vegetation on long-term weathering rates at the Hubbard Brook Experimental Forest, New Hampshire, USA. Geochim. Cosmochim. Acta 68 (14), 3065–3078. https://doi.org/10.1016/j.gca.2004.01.021.
Nezat, C.A., Blum, J.D., Yanai, R.D., Hamburg, S.P., Filippelli, G., 2007. A sequential extraction to determine the distribution of apatite in granitoid soil mineral pools with application to weathering at the Hubbard Brook Experimental Forest, NH, USA. Appl. Geochem. 22, 2406–2421. https://doi.org/10.1016/j.apgeochem.2007.06.012.
Oh, N.H., Hofmockel, M., Lavine, M.L., Richter, D.D., 2007. Did elevated atmospheric CO2 alter soil mineral weathering?: An analysis of 5-year soil water chemistry data at Duke FACE study. Glob. Chang. Biol. 13 (12), 2626–2641. https://doi.org/10.1111/j.1365-2486.2007.01452.x.
Olorunfemi, I.E., Fasinmirin, J.T., Akinola, F.F., 2018. Soil physico-chemical properties and fertility status of long-term land use and cover changes: A case study in forest vegetative zone of Nigeria. Eurasian Journal of Soil Science 7 (2), 133–150. https://doi.org/10.18393/ejss.366168.
Orton, T.G., Pringle, M.J., Bishop, T.F.A., 2016. A one-step approach for modelling and mapping soil properties based on profile data sampled over varying depth intervals. Geoderma 262, 174–186. https://doi.org/10.1016/j.geoderma.2015.08.013.
Oursin, M., Pierret, M.C., Beaulieu, É., Daval, D., Legout, A., 2023. Is there still something to eat for trees in the soils of the Strengbach catchment? For. Ecol. Manage. 527. https://doi.org/10.1016/j.foreco.2022.120583.
Paul, E.A., 2016. The nature and dynamics of soil organic matter: Plant inputs, microbial transformations, and organic matter stabilization. In: Soil Biology and Biochemistry, Vol. 98. Elsevier Ltd., pp. 109–126. https://doi.org/10.1016/j.soilbio.2016.04.001
Pichler, V., Gömöryová, E., Leuschner, C., Homolák, M., Abrudan, I.V., Pichlerová, M., Střelcová, K., Di Filippo, A., Sitko, R., 2021. Parent material effects on soil organic carbon concentration under primeval european beech forests at a regional scale. Forests 12 (4). https://doi.org/10.3390/f12040405.
Porter, V.M., Shanley, J.B., Sebestyen, S.D., Liu, F., 2022. Controls on decadal, annual, and seasonal concentration-discharge relationships in the Sleepers River Research Watershed, Vermont, northeastern United States. Hydrol. Process. 36 (3). https://doi.org/10.1002/hyp.14559.
R Core Team (2023). R: A language and environment for statistical computing. R Foundation for Statistical Computing, Vienna, Austria. URL https://www.R-project.org/.
Ratcliffe, N.M., Stanley, R.S., Gale, M.H., Thompson, P.J., Walsh, G.J., 2011. Bedrock geologic map of Vermont: U.S. Geological Survey Scientific Investigations Map 3184, 3 sheets, scale 1:100,000.
Richard, R., Kane, E., Bronson, D., Kolka, R., 2022. Whole-Tree Harvest Effects on Macronutrients in an Oak-Dominated System after Seven Years. Forests 13 (10). https://doi.org/10.3390/f13101532.
Richardson, J.B., Friedland, A.J., 2016. Influence of coniferous and deciduous vegetation on major and trace metals in forests of northern New England, USA. Plant and Soil 402 (1–2), 363–378. https://doi.org/10.1007/s11104-016-2805-5.
Richardson, J.B., King, E.K., 2018. Regolith weathering and sorption influences molybdenum, vanadium, and chromium export via stream water at four granitoid Critical Zone Observatories. Front. Earth Sci. 6. https://doi.org/10.3389/feart.2018.00193.
Richardson, J.B., Petrenko, C.L., Friedland, A.J., 2017. Base cations and micronutrients in forest soils along three clear-cut chronosequences in the northeastern United States. Nutr. Cycl. Agroecosyst. 109 (2), 161–179. https://doi.org/10.1007/s10705-017-9876-4.
Richardson, J.B., Zuñiga, L.X., 2021. Quantifying aluminosilicate manganese release and dissolution rates across organic ligand treatments for rocks, minerals, and soils. Acta Geochim. https://doi.org/10.1007/s11631.
Righi, D., Meunier, A., 1991. Characterization and genetic interpretation of clays in an acid brown soil (Dystrochrept) developed in a granitic saprolite. Clay Clay Miner. 39, 519–530.
Rogers, N.S., D'amato, A.W., Leak, W.B., 2021. Long-term evolution of composition and structure after repeated group selection over eight decades. Can. J. For. Res. 51 (7), 1080–1091. https://doi.org/10.1139/cjfr-2020-0339.
Rout, G.R., Sahoo, S., 2015. Role of Iron in Plant Growth and Metabolism. Reviews in Agricultural Science 3, 1–24. https://doi.org/10.7831/ras.3.1.
Roy, M.È., Surget-Groba, Y., Delagrange, S., Rivest, D., 2021. Legacies of forest harvesting on soil properties along a chronosequence in a hardwood temperate forest. For. Ecol. Manage. 496. https://doi.org/10.1016/j.foreco.2021.119437.
Safonov, O.G., Bindi, L., Vinograd, V.L., 2011. Potassium-bearing clinopyroxene: a review of experimental, crystal chemical and thermodynamic data with petrological applications. Mineral. Mag. 75 (4), 2467–2484. https://doi.org/10.1180/minmag.2011.075.4.2467.
Schaberg, P.G., Tilley, J.W., Hawley, G.J., DeHayes, D.H., Bailey, S.W., 2006. Associations of calcium and aluminum with the growth and health of sugar maple trees in Vermont. For. Ecol. Manage. 223 (1–3), 159–169. https://doi.org/10.1016/J.FORECO.2005.10.067.
Schachtman, D.P., Reid, R.J., Ayling, S.M., 1998. Update on Phosphorus Uptake Phosphorus Uptake by Plants: From Soil to Cell. Plant Physiol. 116, 447–453. https://academic.oup.com/plphys/article/116/2/447/6085629.
Schattman, R.E., Jean, H., Faulkner, J.W., Maden, R., McKeag, L., Nelson, K.C., Grubinger, V., Burnett, S., Erich, M.S., Ohno, T., 2023. Effects of irrigation scheduling approaches on soil moisture and vegetable production in the Northeastern U.S.A. Agric Water Manag 287. https://doi.org/10.1016/j.agwat.2023.108428.
Soil Survey Staff, Natural Resources Conservation Service, United States Department of Agriculture. Web Soil Survey. Available online. Accessed September 4, 2023.
St. Clair, S.B., Sharpe, W.E., Lynch, J.P., 2008. Key interactions between nutrient limitation and climatic factors in temperate forests: A synthesis of the sugar maple literature. Can. J. For. Res. 38 (3), 401–414. https://doi.org/10.1139/X07-161.
Street, B.B., Rice, A.M., Richardson, J.B., 2023. Forest floor and Na azide effect on elements in leachate from contrasting New Hampshire and Virginia forest soils. Soil Sci. Soc. Am. J. 87 (6), 1444–1457. https://doi.org/10.1002/saj2.20580.
Sulieman, M., Saeed, I., Hassaballa, A., Rodrigo-Comino, J., 2018. Modeling cation exchange capacity in multi geochronological-derived alluvium soils: An approach

based on soil depth intervals. Catena 167, 327–339. https://doi.org/10.1016/j.catena.2018.05.001.
Tessier, A., Campbell, C.P.G., Bisson, M., 1979. Sequential extraction procedure for the speciation of particulate trace metals. Anal. Chem. 51 (7), 844–851. https://pubs.acs.org/sharingguidelines.
Tunesi, S., Poggi, V., Gessa, C., 1999. Phosphate adsorption and precipitation in calcareous soils: the role of calcium ions in solution and carbonate minerals. In Nutrient Cycling in Agroecosystems (Vol. 53).
U.S. Geological Survey, Aziscohos Formation, Lower unnamed member at https://mrdata.usgs.gov/geology/state/sgmc-unit.php?unit=NHOCAzl%3B0. (Accessed September 7, 2023).
U.S. Geological Survey, Waits River Formation- Carbonaceous phyllite and limestone member at https://mrdata.usgs.gov/geology/state/sgmc-unit.php?unit=VTDSw%3B0. (Accessed September 7, 2023).
Vadeboncoeur, M.A., Hamburg, S.P., Yanai, R.D., Blum, J.D., 2014. Rates of sustainable forest harvest depend on rotation length and weathering of soil minerals. For. Ecol. Manage. 318, 194–205. https://doi.org/10.1016/j.foreco.2014.01.012.
Van Breemen, N., Finzi, A. C., Canham, C. D., 1997. Canopy tree-soil interactions within temperate forests: effects of soil elemental composition and texture on species distributions 1.
Velbel, M.A., 1993. Constancy of silicate-mineral weathering-rate ratios between natural and experimental weathering: implications for hydrologic control of differences in absolute rates. Chem. Geol. 105, 89–99.
Wacket, A.A., Yoo, K., Amundson, R., Heimsath, A.M., Jelinski, N.A., 2018. Climate controls on coupled processes of chemical weathering, bioturbation, and sediment transport across hillslopes. Earth Surf. Proc. Land. 43 (8), 1575–1590.
Walmsley, J.D., Jones, D.L., Reynolds, B., Price, M.H., Healey, J.R., 2009. Whole tree harvesting can reduce second rotation forest productivity. For. Ecol. Manage. 257 (3), 1104–1111. https://doi.org/10.1016/j.foreco.2008.11.015.
Walthert, L., Graf Pannatier, E., Meier, E.S., 2013. Shortage of nutrients and excess of toxic elements in soils limit the distribution of soil-sensitive tree species in temperate forests. For. Ecol. Manage. 297, 94–107. https://doi.org/10.1016/j.foreco.2013.02.008.
Wang, Z., Hassan, M.U., Nadeem, F., Wu, L., Zhang, F., Li, X., 2020. Magnesium Fertilization Improves Crop Yield in Most Production Systems: A Meta-Analysis. Front. Plant Sci. 10 (January), 1–10. https://doi.org/10.3389/fpls.2019.01727.
White, A.F., Brantley, S.L., 2003. The effect of time on the weathering of silicate minerals: Why do weathering rates differ in the laboratory and field? Chem. Geol. 202 (3–4), 479–506. https://doi.org/10.1016/j.chemgeo.2003.03.001.
White, P.J., Broadley, M.R., 2003. Calcium in plants. In Annals of Botany (vol. 92 (4), 487–511. https://doi.org/10.1093/aob/mcg164.
Wilson, S.G., Dahlgren, R.A., Margenot, A.J., Rasmussen, C., O'Geen, A.T., 2022. Expanding the Paradigm: The influence of climate and lithology on soil phosphorus. Geoderma 421. https://doi.org/10.1016/j.geoderma.2022.115809.
Woodruff, L., Cannon, W.F., Smith, D.B., Solano, F., 2015. The distribution of selected elements and minerals in soil of the conterminous United States. J. Geochem. Explor. 154, 49–60. https://doi.org/10.1016/j.gexplo.2015.01.006.
Xia, R., Zhang, S.Q., Li, J., Li, H., Ge, L.S., Yuan, G.L., 2023. Spatial distribution and quantitative identification of contributions for nutrient and beneficial elements in top- and sub-soil of Huairou District of Beijing, China. Ecol. Indic. 154. https://doi.org/10.1016/j.ecolind.2023.110853.
Zhang, Y., Rimstidt, D.J., Huang, Y., Zhu, C., 2019. Kyanite far from equilibrium dissolution rate at 0–22 °C and pH of 3.5–7.5. Acta Geochim. 38 (4), 472–480. https://doi.org/10.1007/s11631-019-00347-9.